

TABLE OF CONTENTS

<u>Section</u>	<u>Page</u>
SUMMARY	1 1/A10
1. INTRODUCTION	2 1/A11
2. PROBLEM DEFINITION	4 1/A13
2.1 Description of the Flight Task	4 1/A13
2.2 Control Wheel Steering	4 1/A13
2.3 Displays	5 1/A14
2.4 Simulated Winds	9 1/B4
3. MODEL ANALYSIS	13 1/B8
3.1 Pilot-Related Model Parameters	13 1/B8
3.2 Wind Model	19 1/B14
3.3 Model Predictions	22 1/C3
4 EXPERIMENTAL STUDY	49 1/E2
4.1 Description of Experiments	49 1/E2
4.2 Data Analysis Procedures	50 1/E3
4.3 Comparison of Predicted and Experimental Results	52 1/E5
4.4 Post-Experimental Model Analysis	65 1/F4
5 SUMMARY AND CONCLUSIONS	76 1/G1
APPENDIX	A1 1/G5
Model for Pilot Response to Nonrandom Inputs	
REFERENCES	

AUG 14 1978

celem 830-H-14

NAS1-26:3034

NASA Contractor Report 3034

**ORIGINAL
COMPLETED**

**Analysis and In-Simulator Evaluation
of Display and Control Concepts
for a Terminal Configured
Vehicle in Final Approach
in a Windshear Environment**

William H. Levison

**CONTRACT NAS1-13842
AUGUST 1978**

NASA

102

Item 830-H-14

NAS1.26:3034

NASA Contractor Report 3034

**Analysis and In-Simulator Evaluation
of Display and Control Concepts
for a Terminal Configured
Vehicle in Final Approach
in a Windshear Environment**

William H. Levison
Bolt Beranek and Newman Inc.
Cambridge, Massachusetts

Prepared for
Langley Research Center
under Contract NAS1-13842



**National Aeronautics
and Space Administration**

**Scientific and Technical
Information Office**

1978

BLANK PAGE

LIST OF FIGURES

<u>Figure</u>		<u>Page</u>
1.	Linear Approximation to Control Wheel Steering. . . .	6
2.	Sketch of the EADI Display.	7
3.	Windshear Profile	12
4.	Effect of Display on Predicted Mean Height Error, Shear 1.	25
5.	Effect of Display on Predicted Mean Height Error, Shear 3.	26
6.	Effect of Display on Predicted Mean Airspeed Error, Shear 1.	28
7.	Effect of Display on Predicted Mean Airspeed Error, Shear 3.	29
8.	Effect of CWS on Predicted Mean Height Error, Shear 1.	30
9.	Effect of CWS on Predicted Mean Height Error, Shear 3.	31
10.	Effect of CWS on Predicted Mean Airspeed Error, Shear 1.	33
11.	Effect of CWS on Predicted Mean Airspeed Error, Shear 3.	34
12.	Mean and Standard Deviation for Predicted Height Error.	35
13.	Mean and Standard Deviation of Predicted Airspeed Error.	36
14.	Effect of Display on Predicted Mean Thrust Deviation	38
15.	Effect of Display on Speed Estimation Capability. . .	39
16.	Effect of Reduced Threshold for Perception of Airspeed Error.	41

<u>Figure</u>		<u>Page</u>
17.	Effect of Display on Predicted Ability to Estimate Longitudinal Wind Component.	42
18.	Effect of Display on Predicted Ability to Estimate Vertical Wind Component.	43
19.	Effect of Display on Predicted Mean Error, Shear 3 with Downdraft.	45
20.	Effect of Explicit Display of Wind on Predicted Mean Height Error	46
21.	Effect of Explicit Display of Wind on Predicted Mean Airspeed Error	47
22.	Effect of Display on Mean Height Error, Shear 1	54
23.	Effect of Display on Mean Height Error, Shear 3	55
24.	Effect of Display on Mean Airspeed Error, Shear 1	56
25.	Effect of Display on Mean Airspeed Error, Shear 3	57
26.	Effect of CWS on Mean Height Error, Shear 1	59
27.	Effect of CWS on Mean Height Error, Shear 3	60
28.	Effect of CWS on Mean Airspeed Error, Shear 1	61
29.	Effect of CWS on Mean Airspeed Error, Shear 3	62
30.	Mean and Standard Deviation of Experimental Height Error.	63
31.	Mean and Standard Deviation of Experimental Airspeed Error.	64

<u>Figure</u>		<u>Page</u>
32.	Effect of Display on Predicted Mean Error, Low Threshold for Airspeed Perception.	66
33.	Predicted Response Variability for High Noise/Signal Ratio	68
34.	Effect of Display on Predicted Mean Error, Increased Noise/Signal Ratio	69
35.	Predicted Response Variability for Increased Pilot Uncertainty.	71
36.	Effect of Display on Mean Response for Increased Pilot Uncertainty.	72
37.	Predicted Response Variability for Increased Driving Noise.	74
38.	Effect of Display on Predicted Mean Error for Increased Driving Noise.	75

LIST OF TABLES

<u>Table</u>	<u>Page</u>
1. Limits and Cost Weightings of Model Analysis.	15
2. Display-Related Model Parameters.	16
3. Results of Preliminary Steady-State Analysis.	23
4. Data Base	51

SYMBOLS

FD	flight director error indication, degrees
h	height error, meters
q	pitch rate, degrees/sec
u	aircraft forward velocity relative to still air, meters/second
u_i	indicated airspeed, meters/second
y	output (or display) vector
α	angle of attack error, degrees
γ	vertical path angle error, degrees
γ_{pot}	"potential gamma", degrees
δ_e	elevator deflection, deviation from trim, degrees
δ_{ep}	pilot's control input to elevator, degrees
δ_T	thrust deviation from trim, newtons
θ	pitch deviation from trim, degrees

ACRONYMS

ACWS	attitude control wheel steering
EADI	electronic attitude director indicator
TCV	terminal configured vehicle
VCWS	velocity control wheel steering

SUMMARY

The effects of display and control parameters on approach performance of a simulated Terminal Configured Vehicle (TCV) were explored experimentally in a manned simulation study and analytically using a state-of-the-art pilot/vehicle model. A revised treatment of nonrandom inputs was incorporated in the model. Response behavior was observed for two display configurations (an "advanced" presentation and a flight-director configuration requiring use of a panel-mounted airspeed indicator), two control configurations (attitude and velocity control wheel steering), and two shear environments each of which contained a head-to-tail shear and a vertical component.

In general, performance trends predicted by the model were confirmed experimentally. Experimental and analytical results both indicated superiority of the advanced display with respect to regulation of height and airspeed errors. Velocity steering allowed tighter regulation of height errors, but control parameters had little influence on airspeed regulation. Model analysis indicated that display-related differences could be ascribed to differences in the quality of speed-related information provided by the two displays.

Model predictions were most accurate with regard to the effects of control and display parameters on the total swing of the mean error trajectory over the course of the approach, and least accurate with regard to response variability, which was underestimated by the model predictions. Post-experimental analysis suggested that additional sources of variability not related to inherent pilot response randomness would have to be modeled to improve the match to the data.

1. INTRODUCTION

This report summarizes the second phase of a program to analyze display-control configurations for the Terminal Configured Vehicle (TCV). The work was performed for the National Aeronautics and Space Administration, Langley Research Center (NASA-LRC) under Contract No. NAS1-13842 and was designed to augment a simulation study conducted there.

The first phase of this study explored the effects of certain control and display configurations on approach performance in a zero-mean, random turbulence environment. The LRC simulation study was augmented by an analytic study performed at BBN using a state-of-the-art pilot/vehicle model to explore both performance and workload differences among control/display configurations of interest. The reader is assumed to be familiar with the results of this work and with application of the pilot/vehicle model to TCV approach performance. Frequent reference is made to the report by Levison and Baron [1], which documents the results of the first study phase.

Approach performance of a TCV in windshear environments was studied in the second study phase, with control and display configuration (along with windshear profile) the major variables of interest. The existing pilot/vehicle model was modified to allow a revised treatment of nonrandom inputs; details of this modification are reported in the Appendix to this report. Because the longitudinal and vertical components of the shear have greatest impact on path and airspeed regulation, only longitudinal-axis performance was explored in the analytic study.

The major objective of the model analysis was to provide interpretation of the experimental results, as well as to validate the model in a nonrandom input environment. Nevertheless, the power of such a model is to allow one to explore situations beyond those studied experimentally. Some examples of model extrapolation are given in this report; others are suggested for future study.

In general, the principal trends predicted by the model were confirmed experimentally. As predicted, display parameters influenced the mean time histories of both height and airspeed errors, whereas control parameters influenced primarily regulation of height error. Experimental response variability was substantially greater than predicted, apparently due in part to run-to-run fluctuations in the pilot's subjective performance criteria.

Mr. Samuel Morello directed the manned simulation study, the results of which are analyzed in this report.

2. PROBLEM DEFINITION

2.1 Description of the Flight Task

As in the preceding study phase, the flight task of interest was the standard straight-in (3 degree) approach of a simulated TCV. The vehicle considered was a 737-100 (as simulated at NASA-LRC) with flaps at 40 degrees and gear down. Simulated vehicle weight was 40,824 kg (90,000 lb.), nominal approach speed 61.8 meters/sec (120 kt), and trim angle of attack 4.36 degrees. The simulated atmospheric environment contained low-level zero-mean gusts plus a wind shear consisting of a rotating horizontal component and a brief interlude of either an updraft or a downdraft.

Manual control of the throttle was employed in this study phase (airspeed was regulated by autothrottle in the preceding study phase). Manual control of the elevator was augmented by inner-loop feedbacks provided by the TCV control system as briefly described below.

2.2 Control Wheel Steering

The TCV is equipped with an advanced control system that can operate in the modes known as "Attitude Control Wheel Steering (ACWS) and Velocity Control Wheel Steering (VCWS). Basically, these modes provide attitude-rate stabilization and allow the pilot, in effect, to command either attitude (ACWS) or path angle (VCWS). A more complete description of the control wheel steering is given in Levison and Baron [1].

In order to use the existing man-machine model, the track-hold feature of the CWS was approximated by a continuous, linear feedback law as shown in Figure 1.

2.3 Displays

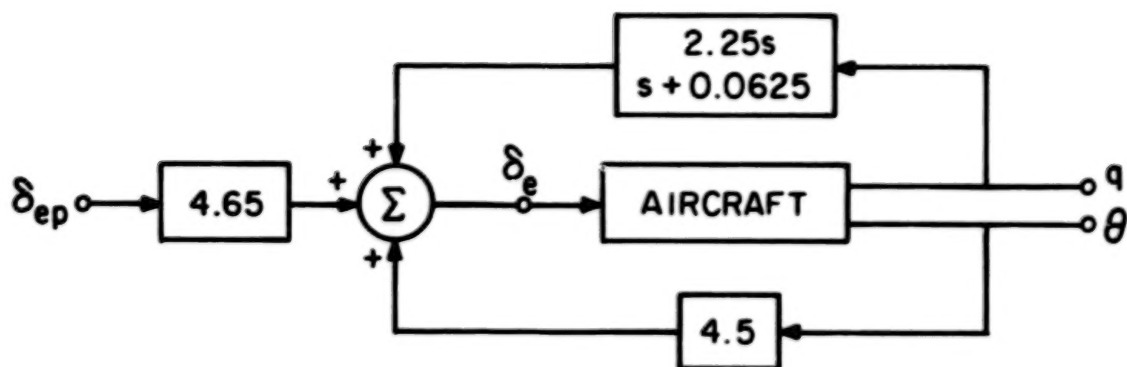
Flight control information was provided primarily by the electronic attitude/director indicator (EADI), a sketch of which is given in Figure 2.

Two display configurations were considered: (1) the "advanced" display, which presented information in an integrated (pictorial) format, and (2) the flight director display, which provided director information based on path, path angle, and attitude errors.

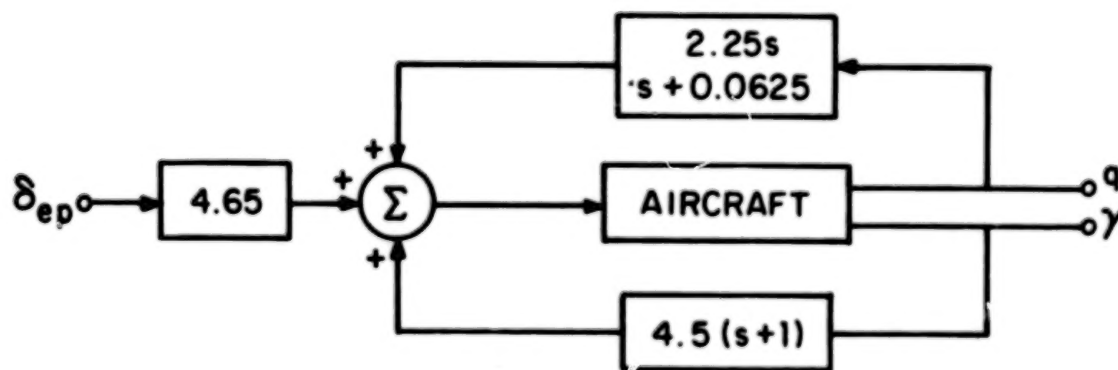
2.3.1 Advanced Display

The advanced display provided the following flight-control information (as diagrammed in Figure 2):

- a. an aircraft symbol to serve as x-axis airframe reference,
- b. an artificial horizon and pitch attitude scale,
- c. a roll attitude scale and pointer,
- d. a pair of so-called "gamma wedges" to indicate path angle,
- e. a dashed line to indicate a point 3 degrees below the horizon,
- f. a perspective runway symbol,



(a) ATTITUDE CWS



(b) VELOCITY CWS

Figure 1. Linear Approximation to Control Wheel Steering

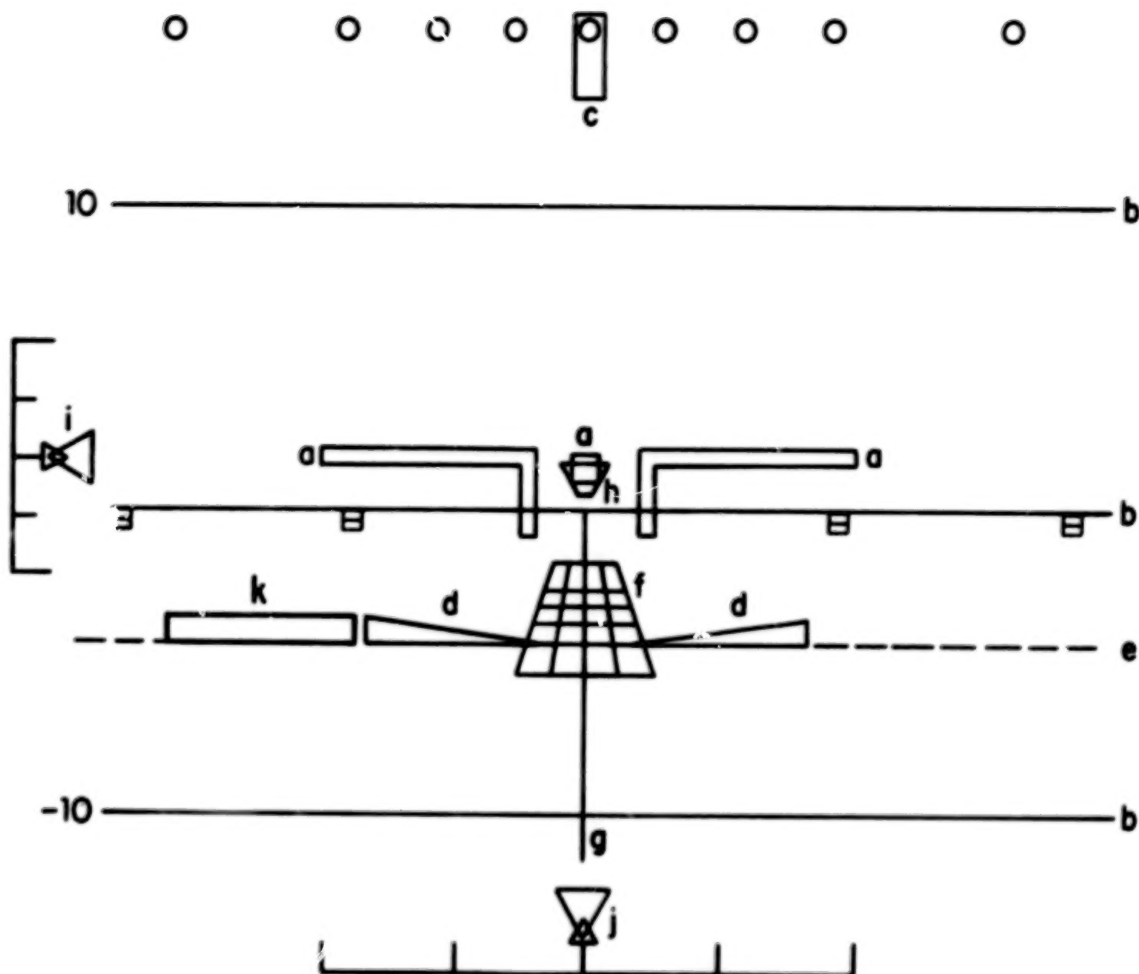


Figure 2. Sketch of the EADI Display
(Display elements defined in the text)

- g. an extended runway center line to aid in lineup regulation,
- h. a symbol to indicate track angle,
- i. a glideslope indicator,
- j. a localizer indicator, and
- k. a so-called "potential gamma" symbol to provide information relative to speed management.

Except for the potential gamma symbol, this display was identical to the advanced display used in the preceding study phase, and the reader is referred to Levison and Baron for additional details on the structure and use of this display.

A weighted sum of airspeed error and rate of change of vehicle velocity was used to drive the potential gamma symbol, relative to the gamma wedge, in the vertical dimension. Specifically, motion of the gamma wedge was described approximately as follows:

$$\gamma_{\text{pot}} - \gamma \approx 0.543 \dot{u} + 0.24 u_i \quad (1)$$

where 1 unit of potential gamma induces the same amount of indicator displacement as 1 degree of pitch (or path angle) error.

2.3.2 Flight Director Display

The "flight director display" consisted of a raw status display plus director information. The EADI provided attitude information, glideslope and localizer errors in symbolic format, and director information. Airspeed and rate-of-climb were displayed by conventional panel meters.

Perspective runway, gamma wedges, and potential gamma were omitted from the EADI in this display configuration.

Director information was provided with a pair of crossbars that deviated from the x-axis reference symbol in a "fly-to" mode. The following approximation was used during model analysis to represent motion of the vertically-moving director element:

$$FD = \left[-2.0q - \frac{0.011}{s+1} h \right] \cdot \frac{1}{s+1.25} - 1.0 \gamma \quad (2)$$

where upward deflection is defined as positive. Director motion was scaled so that one unit of "director error" produced a displacement of the director indicator equal to the displacement of the artificial horizon produced by one degree of attitude error.

2.4 Simulated Winds

Wind shears as well as zero-mean random gusts were simulated in the NASA-LRC experiments. Gusts of 0.3 M/sec (1 ft/sec) were simulated for all three translational axes, with the frequency dependency changing with height as described in Section 4.1. In order to simplify problem formulation and reduce computational requirements, the effects of these simulated gusts were approximated in the model analysis by including wide-band disturbances added in parallel with the control deflections. A comparison of system performance in response to simulated gusts and to the alternative treatment is provided in the following section of this report.

The simulated wind shear used for both the experimental study and model analysis contained a rotating horizontal component plus a brief vertical component. The three components of the shear were generated as follows:

$$\begin{aligned}w_x &= \rho \cos \theta \cos \phi \\w_y &= \rho \sin \theta \cos \phi \\w_z &= \rho \sin \phi\end{aligned}\tag{3}$$

where ρ is the magnitude of the wind, θ is the angle between the projection of the wind onto the horizontal plane and the desired track ($\theta=0$ represents a headwind), and ϕ is the angle between the wind vector and the horizontal plane. The subscripts x,y,z refer to wind components along the track, across the track, and vertical, respectively.

Model predictions were obtained for performance in two shear environments denoted as "Shear 1" and "Shear 3". In both cases, the wind magnitude remained steady at 25 kts for altitudes above some designated height h_{\max} and decreased linearly with altitude to 10 kts at ground level. The horizontal direction θ remained constant for altitude above h_{\max} and varied linearly in a clockwise direction with altitude to touchdown. The vertical directional angle ϕ was zero for most of the approach and took the form of a triangular pulse with regard to the angle θ for a span of about 10° in θ . Shear 1 exhibited a peak head-tail shear of 5.8 kts per 30.5 (100 ft) at an altitude of about 137 M peak head-tail shear for Shear 3 was approximately 8 kts per 30.5M ft. at an altitude of about 152M.

Figure 3 shows the relationship between wind speed and range for points along the nominal 3 degree glide path.* (Note that the horizontal and vertical wind components have been scaled differently in this figure.) With regard to disruption of the height-regulation task, the horizontal and vertical wind components tended to reinforce each other for Shear 1 and tended to cancel each other in Shear 3. Both shears exhibited a head-to-tail component that tended to cause a loss of lift. Shear 1 included a downdraft, whereas Shear 3 contained an updraft which, as we shall show later, tended to correct the altitude error induced by the horizontal shear.

*Since windspeed is an explicit function of altitude, rather than range, deviation of the aircraft from the desired glide path would modify somewhat the range dependency shown in Figure 3.

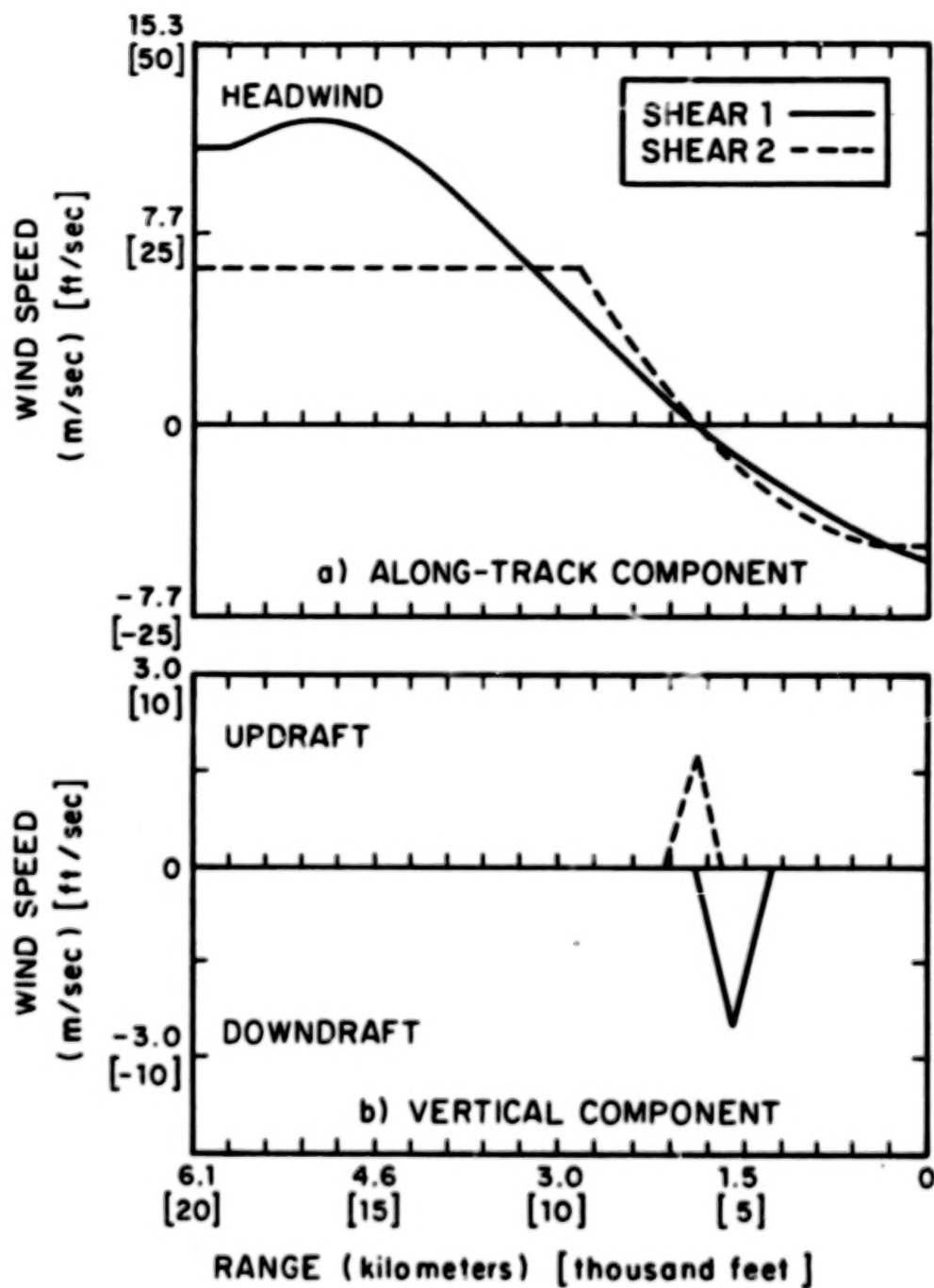


Figure 3. Windshear Profile

3. MODEL ANALYSIS

Prior to analysis of experimental results, the optimal-control pilot/vehicle model was used to predict the effects of control and display configurations on performance in wind shear environments. The model employed in this study was basically the same model employed in the preceding study except for the modified treatment of deterministic inputs as described in the appendix.

A description of the task environment in suitable mathematical format and selection of values for pilot-related model parameters is required to obtain a model solution. The modeling of vehicle dynamics as described in Levison and Baron [1] was modified as indicated in Figure 1 to account for control wheel steering augmentation. Selection of pilot parameters is described below, followed by the treatment of simulated wind disturbances in Section 3.2 and presentation of model results in Section 3.3.

3.1 Pilot-Related Parameters

3.1.1 Cost Weightings

The pilot is assumed to adopt a control strategy that minimizes a weighted sum of mean-squared response variables. In this study, the "cost function" included height error, sink-rate error, airspeed error, angle-of-attack error, control deflection, and rate-of-change of control deflection. Weightings were derived by first associating a maximum allowable value (or "limit") with each variable and then setting the corresponding cost coefficient equal to the square of the reciprocal of the corresponding limit. Limits were selected on the basis of Category II approach specifications (height and airspeed errors),

physical constraints (control-related variables), and assumed pilot preference (sinkrate and angle-of-attack errors).

Analysis of experimental results obtained in the preceding study suggested that pilots tended to regulate height error in terms of an angular, rather than a linear, criterion. Accordingly, the assumed limits on height and sinkrate errors were varied in a piecewise-linear fashion with range as described in Levison and Baron. Limits and weightings for remaining variables were kept fixed throughout the "flight." Limits and weightings used in the model analysis are given in Table 1.

3.1.2 Display-related Parameters

A white Gaussian "observation noise" process is associated with each perceptual variable used by the pilot to account for sources of response randomness related to acquisition and processing of displayed information. The variance of each process is a function of (a) the variance of the signal presented on the display, (b) an associated "threshold" to account for visual resolution limitations and/or pilot indifference to small errors, (c) a "residual noise" to account for loss of perceptual accuracy when a null indicator is lacking, and (d) a "noise/signal ratio" to reflect the amount of central attention devoted to the display variable. The procedure for deriving numerical values for these parameters is discussed in Levison and Baron.

Values for display-related parameters are given in Table 2. When tracking with the advanced display, the pilot was assumed to perceive height error, sinkrate error, pitch and pitch rate, flight path angle and path angle rate, and potential gamma.

Table 1

Limits and Cost Weightings of Model Analysis

a. Range-Varying Experiments

Range (meters)	Nominal Altitude (meters)	Cost Weighting	
		Height Error	Sinkrate Error
6958	364	8.1 E-04	1.3 E-03
4879	255	1.6 E-03	2.6 E-03
3449	180	3.2 E-03	5.1 E-03
2438	128	6.4 E-03	1.0 E-02
1724	90	1.3 E-02	2.0 E-02
1219	64	2.6 E-02	8.9 E-02
862	45	5.2 E-02	8.1 E-02
610	32	1.0 E-02	1.6 E-01
431	23	2.0 E-01	3.2 E-01

b. Range-Invariant Parameters

Variable	Limit	Cost Weighting
u_i	2.6 M/sec	0.15
α	2.0 deg	0.25
δ_e	2.38 deg	0.18
$\dot{\delta}_e$	3.88 deg/sec	0.066
δ_T	37,400 newtons	7.1 E-10
$\dot{\delta}_T$	22,200 newtons/ sec	2.0 E-09

Table 2
Display-Related Model Parameters

Variable	Advanced Display			Director Display		
	a	σ_o	P(dB)	a	σ_o	P(dB)
h	(1)	0	-17	-	-	-
\dot{h}	(2)	0	-17	-	-	-
θ	0.1	1.35	-17	-	-	-
q	0.4	0	-17	-	-	-
γ	0.1	0	-17	-	-	-
$\dot{\gamma}$	0.4	0	-17	-	-	-
γ_{pot}	0.1	0	-17	-	-	-
u_i	-	-	-	1.0	0	-14
FD	-	-	-	0.1	0	-14
\dot{FD}	-	-	-	0.4	0	-14

a = Threshold

σ_o = Residual Noise

P = Noise/Signal Ratio

- indicates variable not observed

(1) Range-varying threshold = $(4.5/1910) * \text{Range}$

(2) Range-varying threshold = $(13/1910) * \text{Range}$

Because movement of the perspective runway with respect to the nominal glideslope was proportional to error in angular terms, the thresholds for height and sinkrate errors (in terms of feet and ft/sec) varied linearly with range. The height error threshold was based on an "indifference threshold" of 1.4 meters at the 30 meter decision height as determined from previous analysis. Other threshold values were based on considerations of visual resolution as described in Levison and Baron. The noise/signal ratio associated with use of the advanced display reflects a moderate-to-high level of workload with no interference among display elements (i.e., we assume integration of the displayed information).

When tracking with the director display, the pilot was assumed to rely primarily on the director symbol and the airspeed indicator for continuous flight-control information, with a negligible amount of time spent scanning the status information for monitoring purposes only. The threshold of 1.0 m/sec. on airspeed was based on the assumption that the pilot was indifferent to airspeed errors smaller than the calibration increments of the airspeed indicator (2 kts); threshold values for perception of director displacement and rate were based on visual resolution limitations. The noise/signal level of -14 dB reflects the same overall level of attention to the task as before, with the requirement to share attention between the director and airspeed indicators. For simplicity, equal sharing of attention between the two displays was assumed, and loss of visual inputs associated with eye movements was neglected.

3.1.3 Other Parameters

Because of the time (range) variations inherent in the nature of the task, a discrete-time formulation of the pilot model was used in this study. An integration time step of 1 second was selected. Although too large to faithfully reproduce high-frequency response behavior in general, this time step was considered adequate to reproduce the essential behavior of the relatively slowly-varying height and speed response of the system to the kinds of windshears explored in this study.*

In order to minimize computational requirements, pilot time delay was ignored (i.e., assumed to be zero). Again, because of the low-frequency nature of the response variables of primary interest, this assumption was considered to have little impact on the trends of the model predictions.

On the basis of previous laboratory results, a motor noise/signal ratio of -25 dB was used to account for motor-related sources of pilot randomness and to reflect uncertainties about the pilot's control response.

Modification of the pilot model resulted in additional parameters related to detection of and response to the windshear. These parameters are discussed below and in the appendix.

*Because computation time for a model solution varies inversely with the integration time step, one is motivated to use as large a time step as possible consistent with the time variations expected for the response variables of major interest.

3.2 Wind Model

The wind environment simulated in the NASA-LRC experimental study included both shear and gust components. Treatments of these inputs in the model analysis are discussed separately below.

3.2.1 Wind Shear

Modeling the pilot's response to a deterministic (i.e., non-zero-mean) input--of which a windshear is an example--involves two basic considerations: (1) the degree to which the pilot understands the nature of the input (i.e., his "internal model"), and (2) the way in which the pilot detects and responds to the input. A brief outline of these considerations is given here; a more detailed exposition of this aspect of the pilot model is given in the appendix.

A simple representation of the pilot's knowledge of the windshear was adopted; basically, we assumed no specific knowledge of the shear, only the knowledge that a non-zero-mean wind might exist. We assumed that the pilot would not try to anticipate changes in the wind, but would, at best, attempt to estimate the current wind vector. This level of pilot knowledge was modeled by simply implementing a stepwise-constant representation of the wind. Since the wind varied relatively slowly with time, the integration time step of 1 second was sufficiently fine to allow an adequate representation of the continuously-varying wind speed.

The pilot/vehicle model was modified to reflect the following assumptions concerning pilot behavior in a non-zero-mean input environment:

- a. The pilot continuously anticipates the behavior of the display variables he is utilizing, given his current estimates of system states and his internal model of system parameters.
- b. The pilot performs a short-term average on the difference between expected and actual behavior of each display variable.
- c. If average prediction error is sufficiently large with respect to the variability of this error, the pilot becomes additionally uncertain about his estimates of system state variables, and he attempts to upgrade these estimates.

Implementing this set of assumptions led to the following additional pilot-related model parameters: (1) the short-term averaging time, (2) the magnitude of the prediction error considered large enough to warrant special action, and (3) specific state variables to which the pilot attributes his uncertainty. In addition, an algorithm had to be formulated for relating prediction errors to increased uncertainty.

Model predictions discussed in the main body of this report were obtained with the assumptions that (1) prediction errors were averaged over about two seconds, (2) an average deviation of two standard deviations from the expected value warranted

special consideration by the pilot, and (3) uncertainty could be associated with any of the principal state variables, including the state variables representing the horizontal and vertical shear components.

3.2.2 Zero-Mean Gusts

The NASA-LRC experimental program with which this analytical effort was associated used first-order noise models to simulate random gusts in each of the three aircraft body axes. Rms levels were fixed at 0.3 m/sec in each axis, but simulated gust bandwidth varied with altitude as described in Section 4.1. The intent of this relatively low-level gust was to keep the pilot active throughout the simulated approach. It was anticipated that the simulated shear would provide the major source of approach-path tracking error.

In order to minimize the order of the overall system dynamics, and thereby minimize computational requirements, this gust model was omitted from the problem description for model analysis. Instead, analysis was performed with simulated white noise disturbances applied to aircraft controls to produce stochastic response behavior similar to that which would have resulted from inclusion of the gust model.

In order to determine proper levels of control disturbance, a steady-state analysis of system response was performed with gusts (but not windshears) simulated. Cost criteria and threshold parameters were selected to reflect pilot response characteristics at a height of 122 meters - an altitude at which head-tail shears were maximal in subsequent approach simulations.

Table 3 compares steady-state model predictions for simulated gusts and for simulated white-noise disturbances having covariances of 0.1 and 2.0×10^8 for noise processes added to δ_{ep} and δ_T , respectively. Predicted rms height, path angle, and throttle deviations differed by about 10 percent for the two simulations. The control-noise simulation yielded a predicted air-speed error of about 75 percent of that predicted by the gust model, and substantially larger differences were observed for predictions of pitch and control-stick activity.

Since the main predictive variables of interest were height and airspeed errors, and since the shear component was assumed to be the main source of tracking error in the approach simulation, the control-noise simulation was considered adequate for predicting the trends of the effects of controls and displays on system performance in windshear environments. This simplified model was used for all subsequent model predictions.

3.3 Model Predictions

Model analysis was performed primarily to explore the effects of alternative display and control configurations on height and airspeed regulation capabilities in two windshear environments. The basic results of this analysis are presented below; additional model results are then presented to explore in further detail the relationship between performance and display properties.

Because of the new treatment of nonrandom inputs, the model used in this study contains certain pilot-related parameters that cannot be adjusted on the basis of past data. Therefore, the model results presented below are not intended to

Table 3

Results of Preliminary Steady-State Analysis

Variable	Predicted RMS Response	
	With Gust Model	With Control Disturbance
h	1.69	1.61
γ	0.202	0.181
θ	0.127	0.286
u_i	0.247	0.190
δ_T	1010	1120
δ_{ep}	0.122	0.0713

predict response behavior with great precision, but rather to indicate important trends related to control and display parameters.

The reader is reminded that the pilot/vehicle model employed in this study predicts the statistical nature of pilot and system performance; that is, a single model run yields predictions of mean response profile as well as the variability about the mean response. Because the wind component of interest (the shear) varies relatively slowly with time, we shall focus mainly on the predicted mean response profile.

3.3.1 Primary Model Results

Presentation of the primary results is organized as follows: (1) effects of display configuration on mean height and airspeed errors, (2) effects of control configuration on these response variables, and (3) sample predictions of response variability.

The effects of display configuration on predicted mean height error are shown in Figure 4 for Shear 1 and Figure 5 for Shear 3. Comparisons of performance with advanced and director displays are shown separately for attitude and velocity CWS. Because the shearing action of Shear 3 did not begin until the simulated aircraft was within 3050 meters of the ILS origin, the range scaling employed in Figure 5 is expanded with respect to the scaling used in Figure 4. Amplitude scaling is the same for both figures.

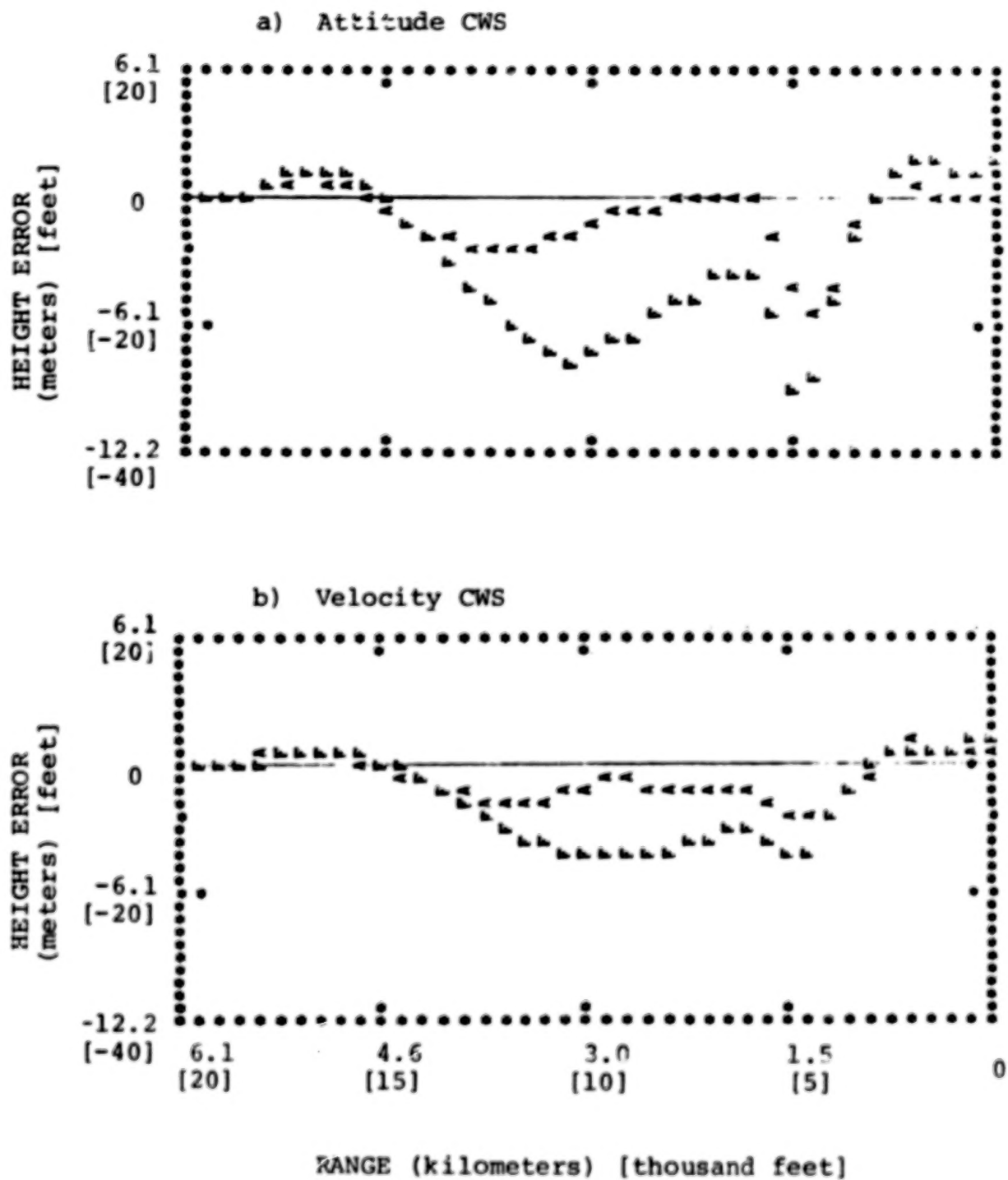


Figure 4. Effect of Display on Predicted Mean Height Error, Shear 1

A = advanced display
F = flight director

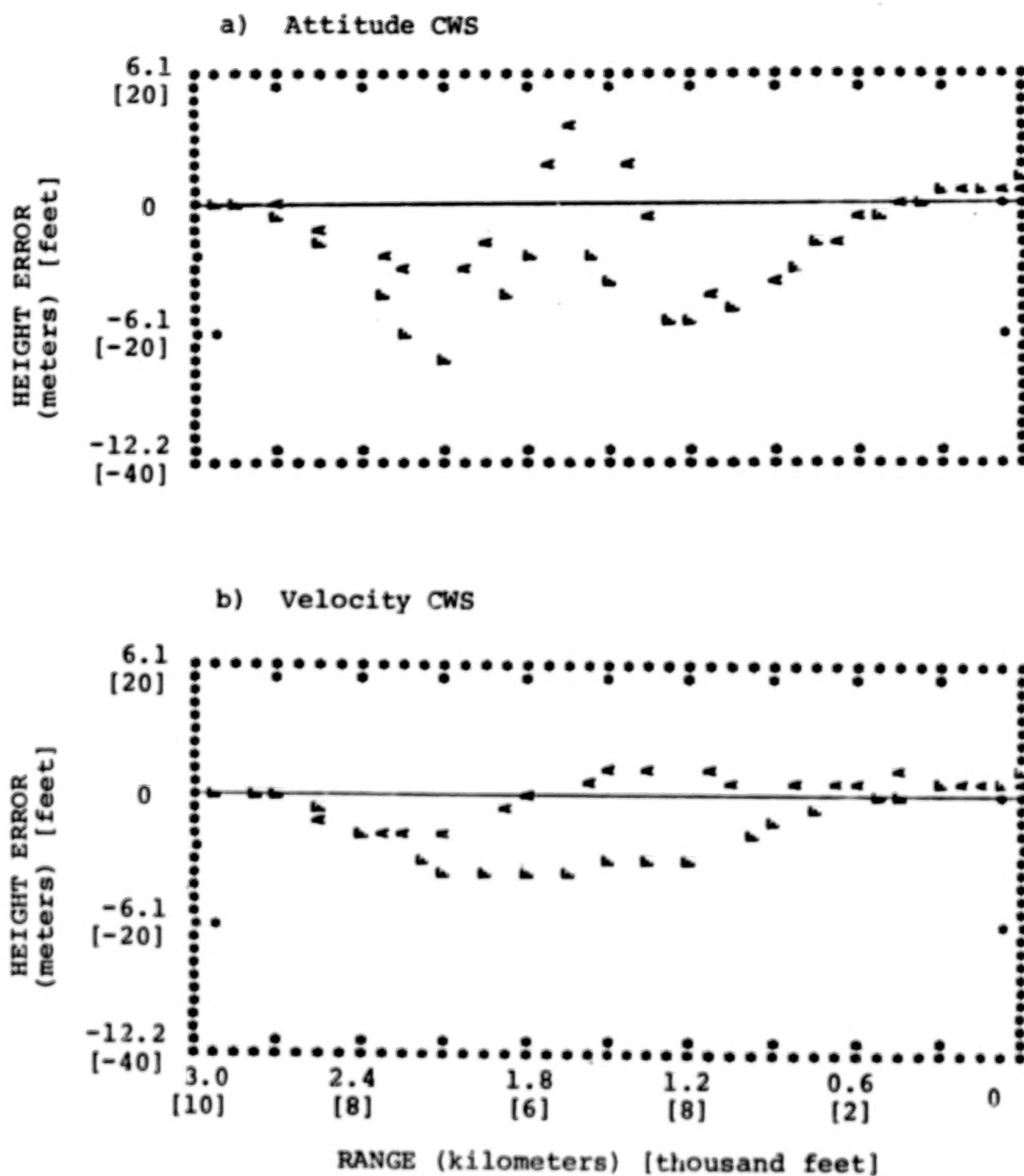


Figure 5. Effect of Display on Predicted Mean Height Error, Shear 3

A = advanced display, F = flight director

Figure 4 shows a consistent trend with regard to display effects; namely, mean height error is substantially greater for the flight director than for the advanced display, with errors generally being negative (i.e., aircraft below the desired glide path).

Figure 5 shows more ambiguous trends for the response to Shear 3. With the attitude CWS mode (Figure 5a), the total swing in predicted mean error over the course of the approach is about the same for the two displays; however, errors with the advanced display are generally more positive than errors with the director display. The oscillatory nature of the height error is caused by the updraft countering the effect of the head-tail shear. Figure 5b (velocity CWS) shows a smoother flight profile, with larger errors predicted for the flight director display.

Figures 6 and 7 show consistent effects of display configuration on predicted airspeed error. In all cases, the director display leads to speed deviations over the course of the approach that are from 2 to 3 times as great as those predicted for the advanced display. For most of the approach, speed errors are negative.

The effects of control wheel steering on predicted mean height and airspeed errors are shown in the subsequent four figures. Figures 8 and 9 show that velocity CWS is expected to allow the pilot to regulate height errors more tightly than with attitude CWS. In the case of Shear 1 (Figure 8), velocity CWS seems particularly useful in regulating against the disruptive effects of the downdraft. (Because of the counteracting influence of the horizontal and vertical shears in the Shear 3 experiments, the beneficial effect of velocity CWS with respect to the updraft is obscured.)

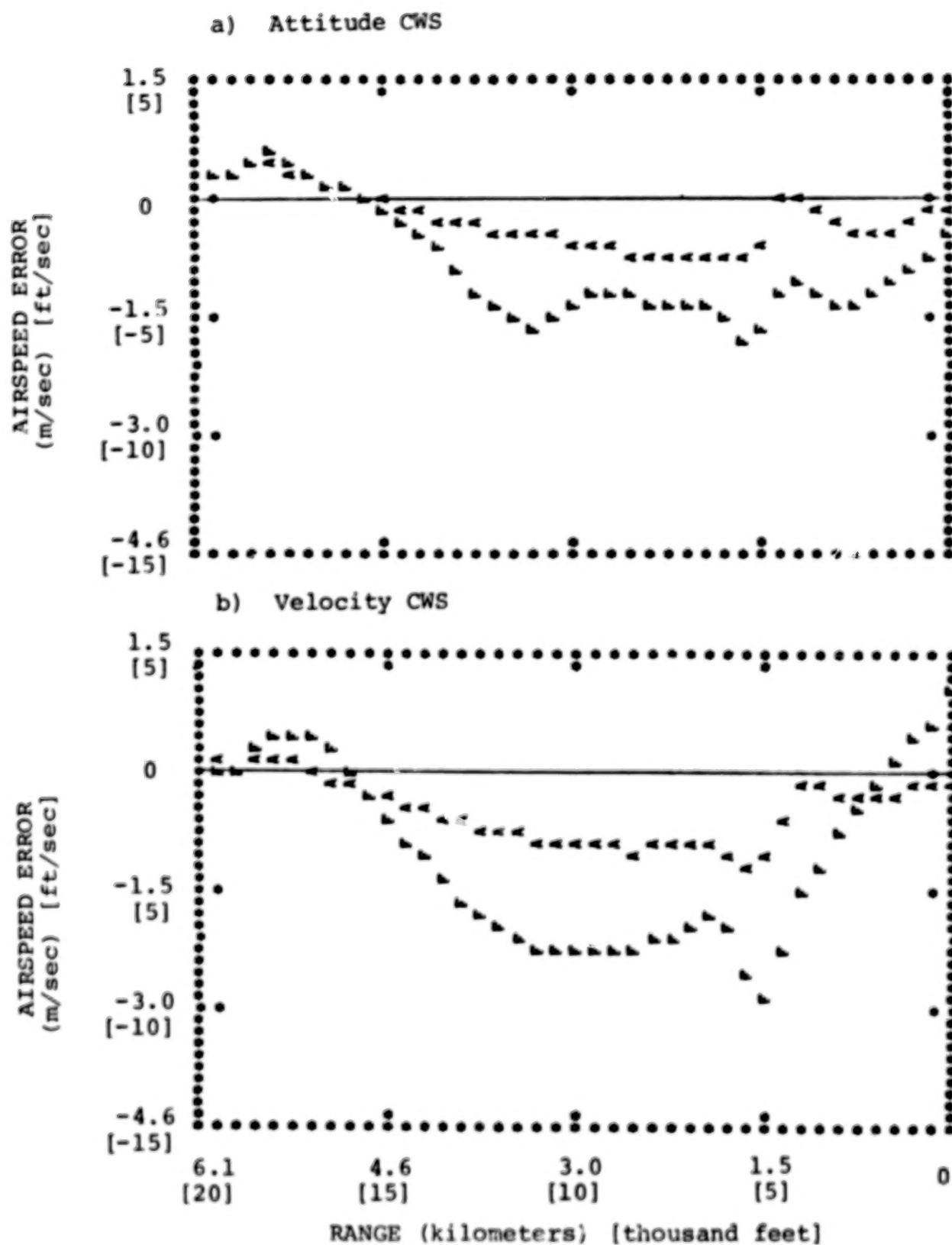


Figure 6. Effect of Display on Predicted Mean Airspeed Error, Shear 1

A = advanced display, F = flight director

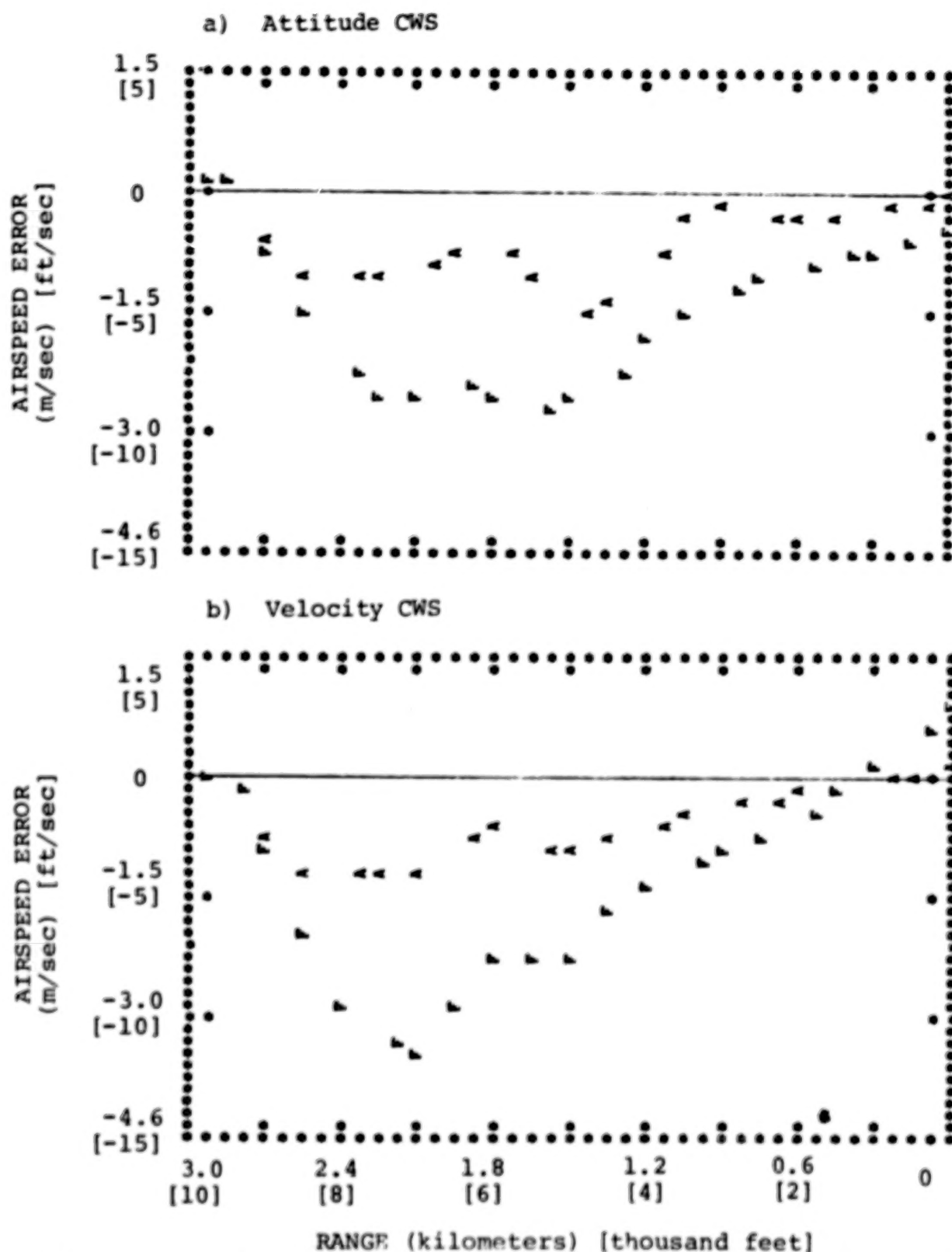
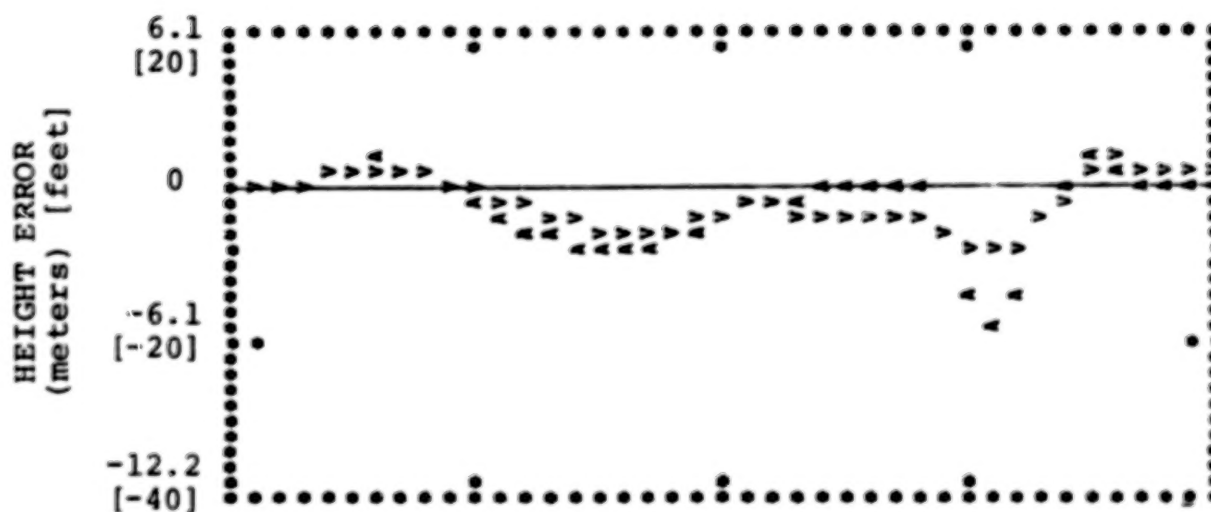


Figure 7. Effect of Display on Predicted Mean Airspeed Error, Shear 3

A = Advanced display, F - flight director

a) Advanced Display



b) Flight Director

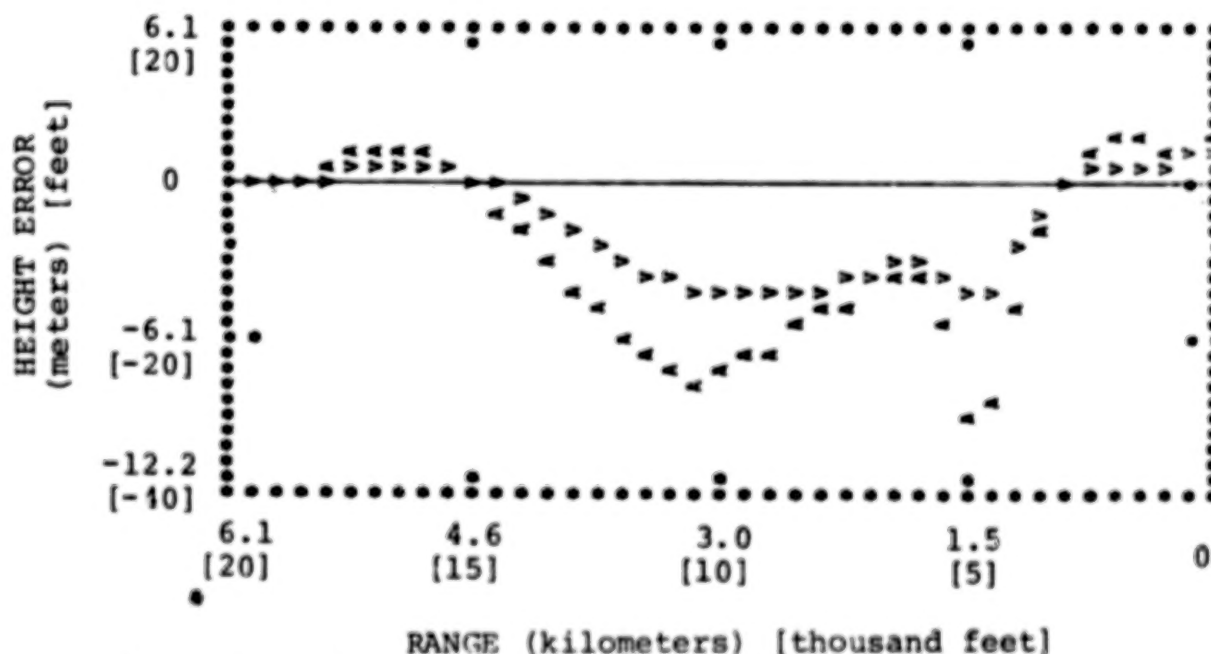


Figure 8. Effect of CWS on Predicted Mean Height Error, Shear 1
A = attitude CWS, V = velocity CWS

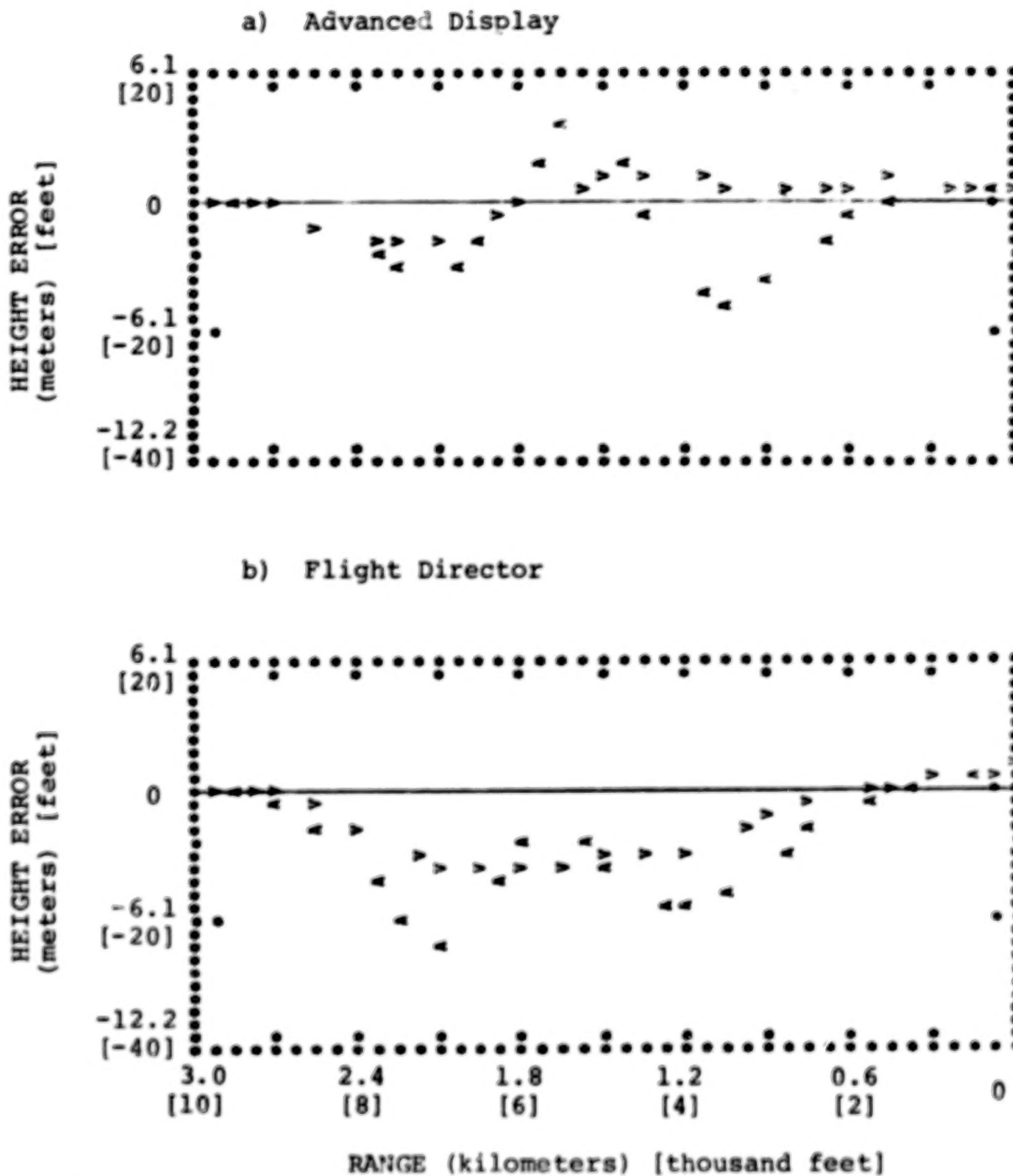


Figure 9. Effect of CWS on Predicted Mean Height Error, Shear 3

A = attitude CWS, V = velocity CWS

Figures 10 and 11 show that, for the most part, control configuration has little effect on predicted mean airspeed error. The only appreciable effect is found for the director display configuration in the Shear 1 environment (Figure 10b), where a noticeable transient drop in airspeed is predicted in the region where the downdraft occurs.

Control/display configuration had little effect on predicted run-to-run variability of either height or airspeed errors. Sample profiles of mean errors and associated 1-sigma envelopes are shown for predicted height and airspeed errors for the advanced display, attitude CWS configuration in Figures 12 and 13.

Figure 12 shows a tendency for the standard deviation of the predicted height error to be largest in the vicinity of maximum predicted mean errors. This trend is seen most clearly for Shear 3 (Figure 12b) which tended to produce larger error variability than Shear 1. In absolute terms the predicted error variability is relatively small, being on the order of 4-6 feet. Modest range-related variations in airspeed variability are also predicted for airspeed error (Figure 13).

To summarize model results so far, display configuration is predicted to influence regulation of both height and airspeed. The advanced display appears to allow tighter control, as larger negative errors and greater swings in expected error over the course of the approach are predicted for the director display. Velocity control wheel steering is predicted to allow tighter regulation of height error, especially in the presence of vertical shears. Control configuration has no consistent effect on predicted airspeed error, however. Controls and displays have little effect on predicted height and speed variability.

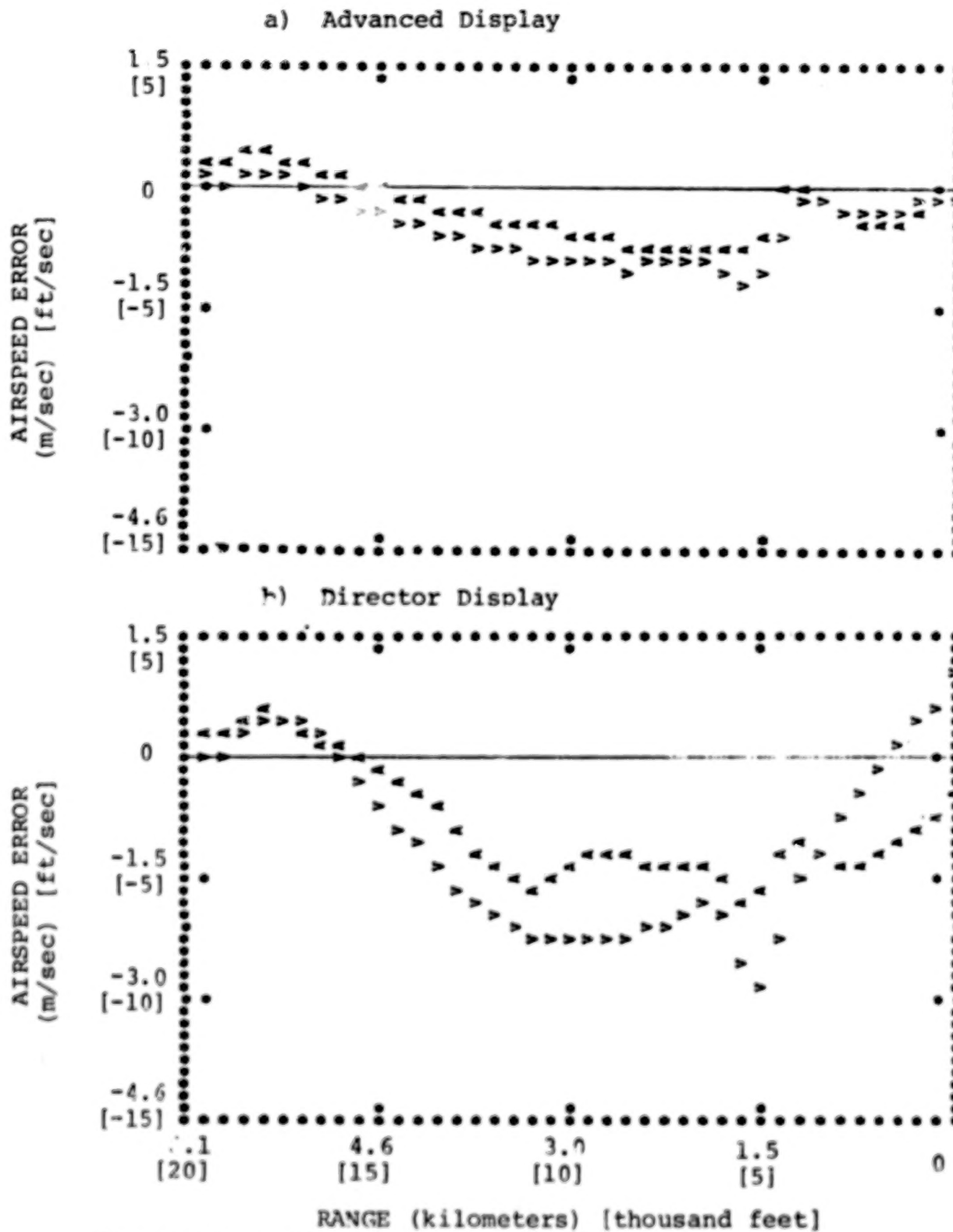


Figure 10. Effect of CWS on Predicted Mean Airspeed Error, Shear 1

A = Attitude CWS, V = Velocity CWS

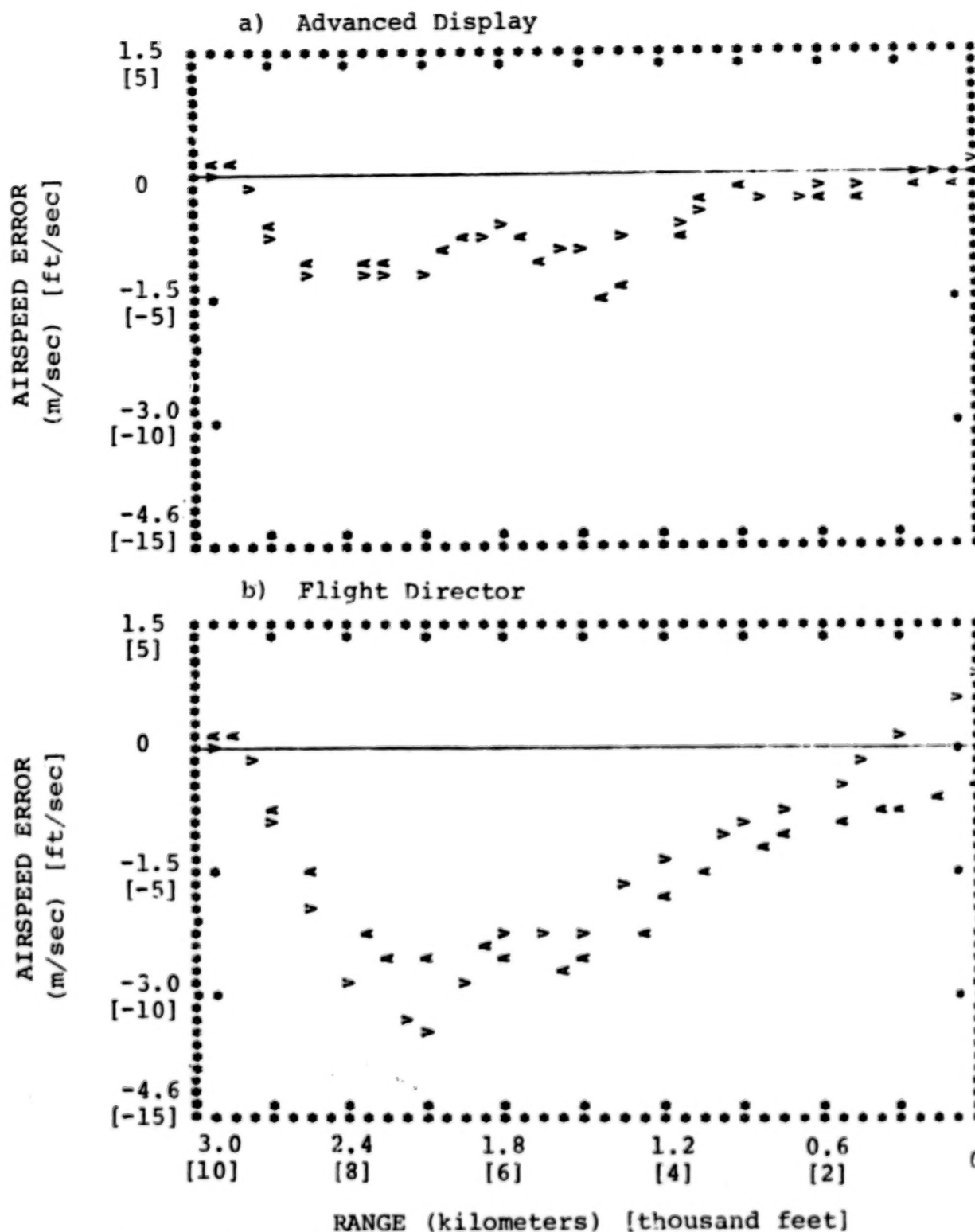


Figure 11. Effect of CWS on Predicted Mean Airspeed Error, Shear 3

A = Attitude CWS, V = Velocity CWS.

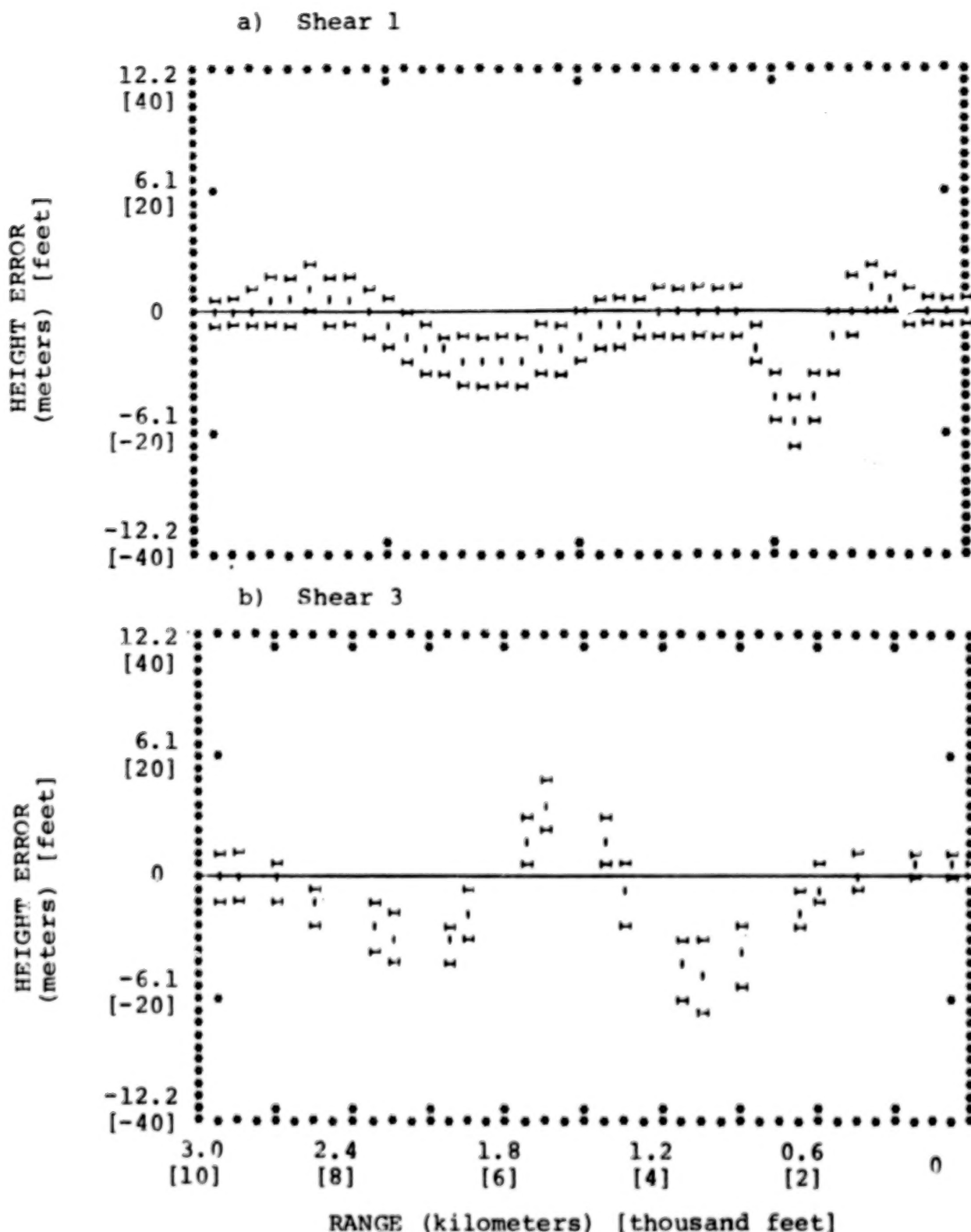


Figure 12. Mean and Standard Deviation for Predicted Height Error
Advanced Display, Attitude CWS.

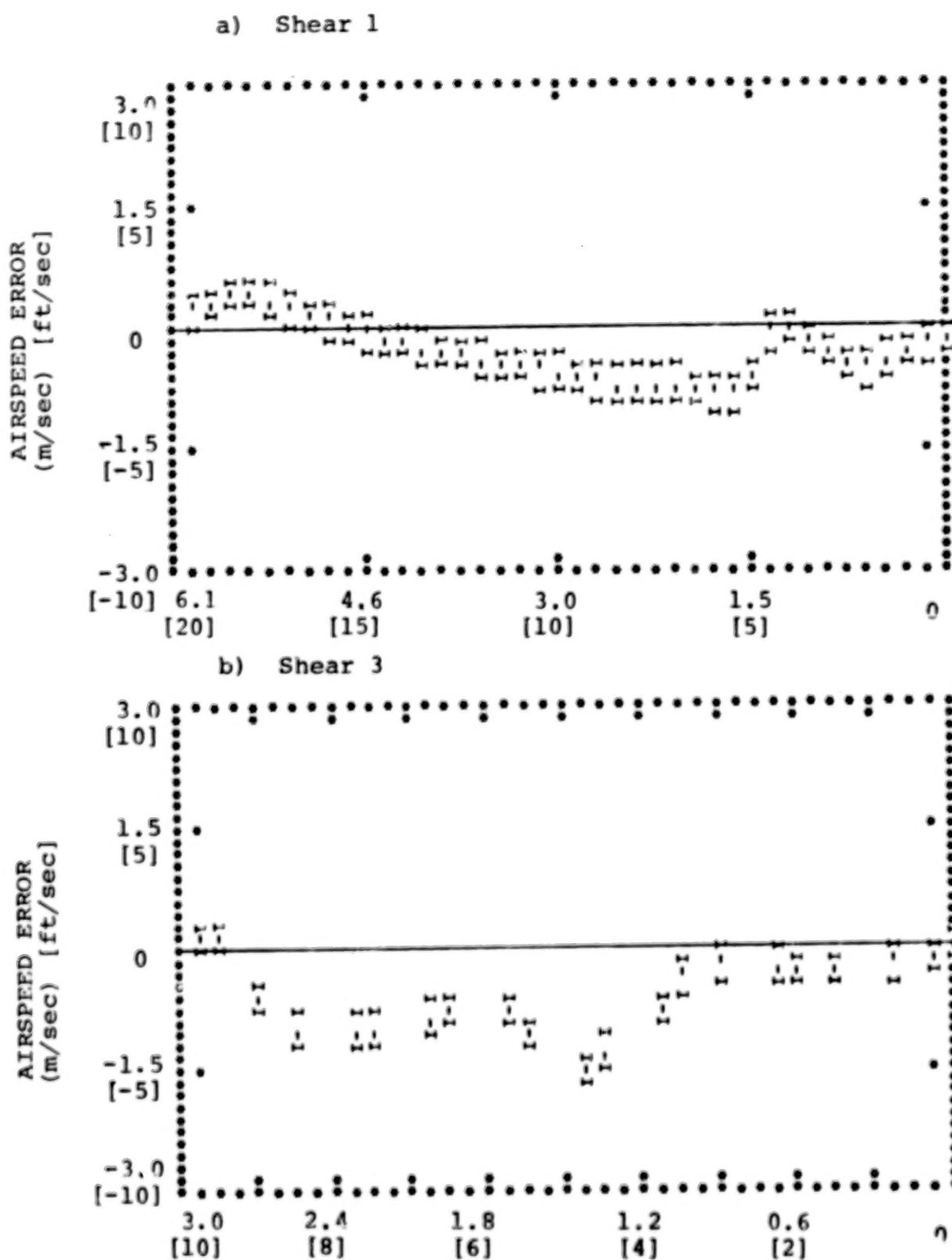


Figure 13. Mean and Standard Deviation of Predicted
Airspeed Error

Advanced display, Attitude CWS

3.3.2 Additional Model Analysis

In the remainder of this chapter on model results we explore potential mechanisms for display-related differences, analyze an additional shear environment, and consider possible display improvements.

Figure 14 shows that predicted throttle response is faster and more vigorous for the advanced than for the director display. (Compare these profiles with corresponding mean air-speed profiles of Figures 6a and 7a.) Presumably, the improved throttle response predicted for the advanced display is a result of the superior speed information provided by this display, as indicated in Figure 15. A comparison of predicted speed error with predicted (pilot) estimate of this error for the Shear 3 environment indicates that the estimate is very close to the actual error when the advanced display is available (Figure 15a). The director display, on the other hand, provides virtually no capability for estimating speed error (Figure 15b).

The poor speed estimation available from the director display configuration is apparently caused by the relatively large threshold assumed for perception of speed error from the (panel) airspeed indicator; predicted estimation capability is greatly improved as this threshold is reduced.

One would expect that the difference in the pilot's ability to obtain speed information accounts at least in part for the predicted display-related differences discussed above. This is not the only potential source of performance difference, however, since suboptimal director laws and scaling could also degrade performance.

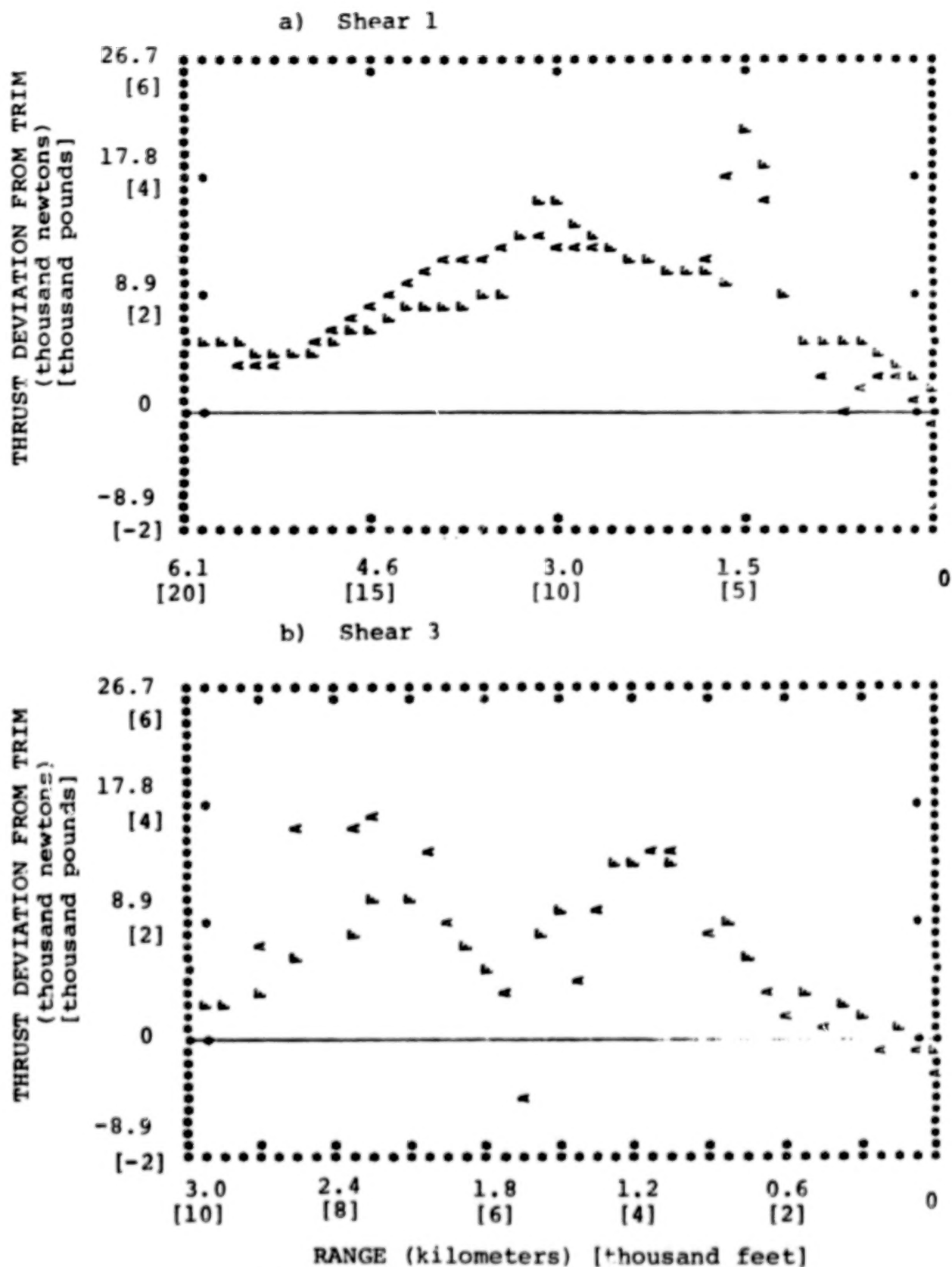


Figure 14. Effect of Display on Predicted Mean Thrust Deviation

Attitude CWS.

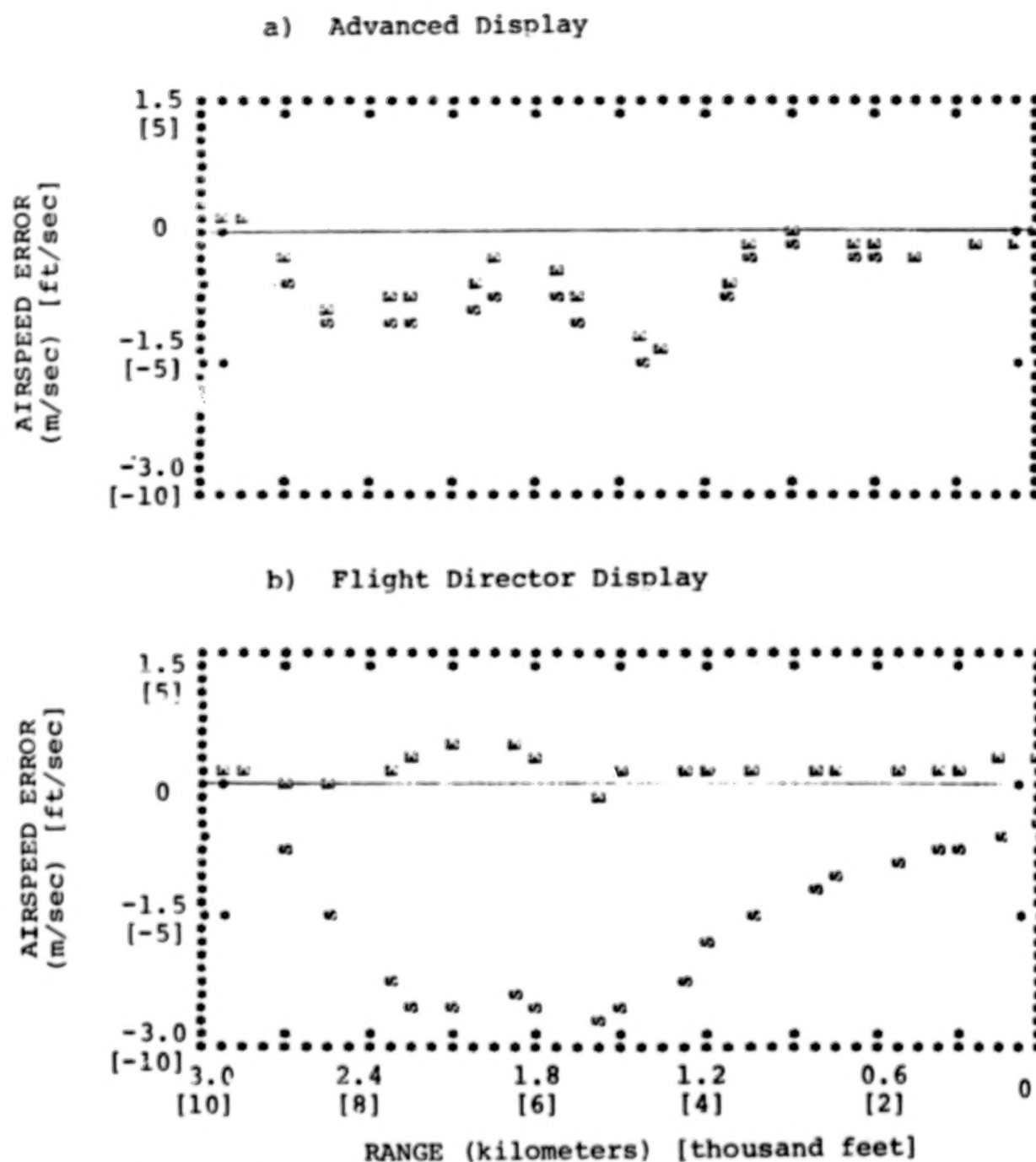


Figure 15. Effect of Display on Speed Estimation Capability

Shear 3, attitude CWS.

S = speed error, E = estimate of speed error.

In order to ascertain the cause of the performance differences predicted for the two display configurations, the director display configuration was reanalyzed with a threshold of 0.024 m/sec (as opposed to 1.0 m/sec assumed previously). This reduced threshold was equivalent to that which would be associated with the potential gamma indicator of the advanced display if potential gamma were driven solely by airspeed error. Director laws and scaling were unchanged, and, as before, the pilot was assumed to share attention equally between the director and speed indicators.

Figure 16 shows that performance with the director display, given improved airspeed resolution, is comparable to that achievable with the advanced display for the Shear 1 environment. There is some tendency to make a different tradeoff between height and speed errors; the revised director display yields somewhat greater height errors and smaller speed errors than those predicted for the advanced display. Quite possibly, revised director laws would yield a different tradeoff between height and speed errors. In any case, reducing the perceptual threshold on airspeed substantially improves performance with the flight director.

Predictions of the pilot's ability to estimate the horizontal and vertical wind components were obtained for the advanced display and for the (unmodified) flight director display. Figures 17 and 18 show that neither display is expected to allow accurate wind estimates, nor is one display consistently superior to the other in this regard. Shortly, we explore the possibility of improving performance via direct display to the pilot of the wind vector.

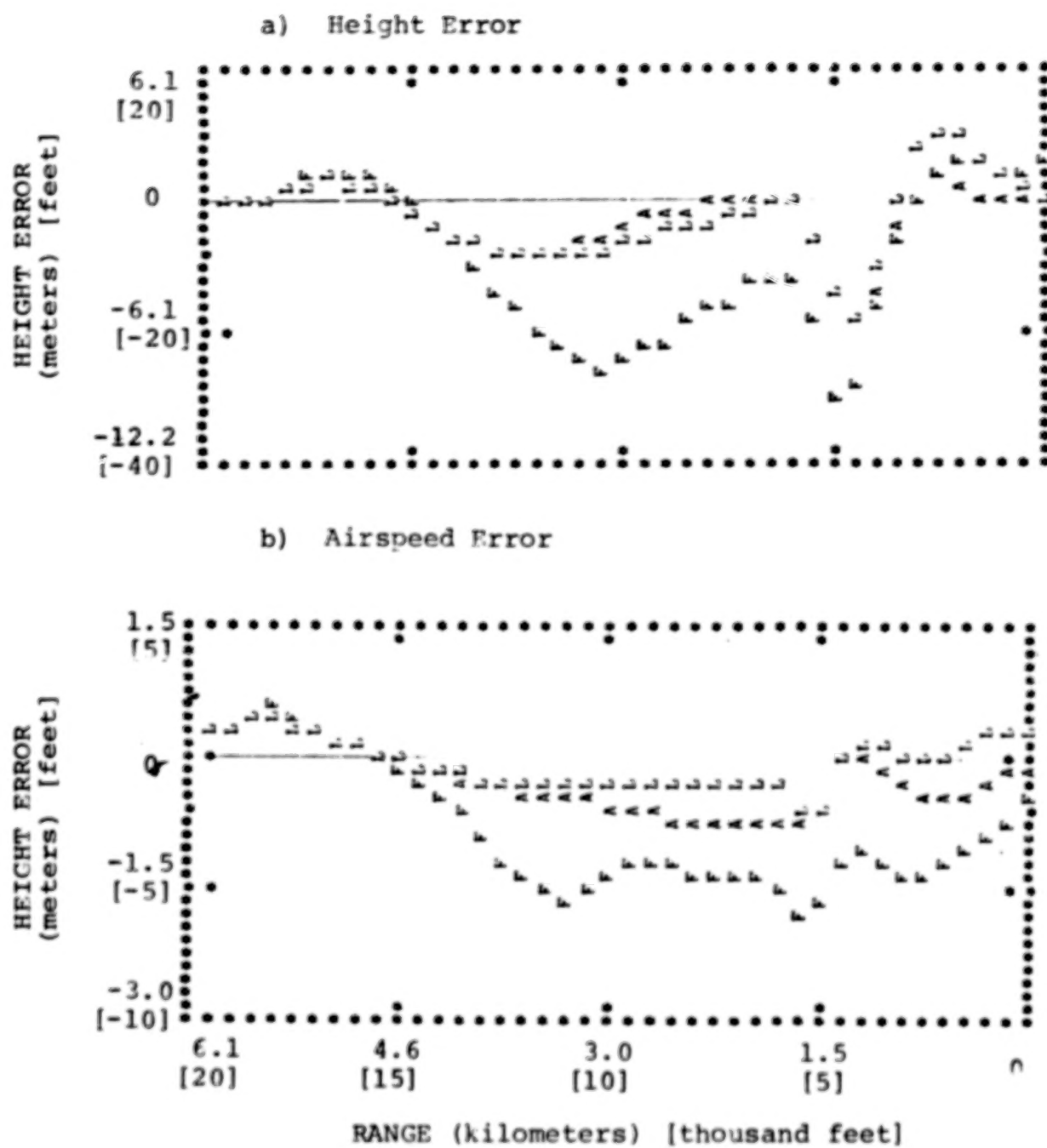


Figure 16. Effect of Reduced Threshold for Perception of Airspeed Error

Shear 1, attitude CWS.

A = advanced display, F = flight director, L = director with lowered perceptual threshold.

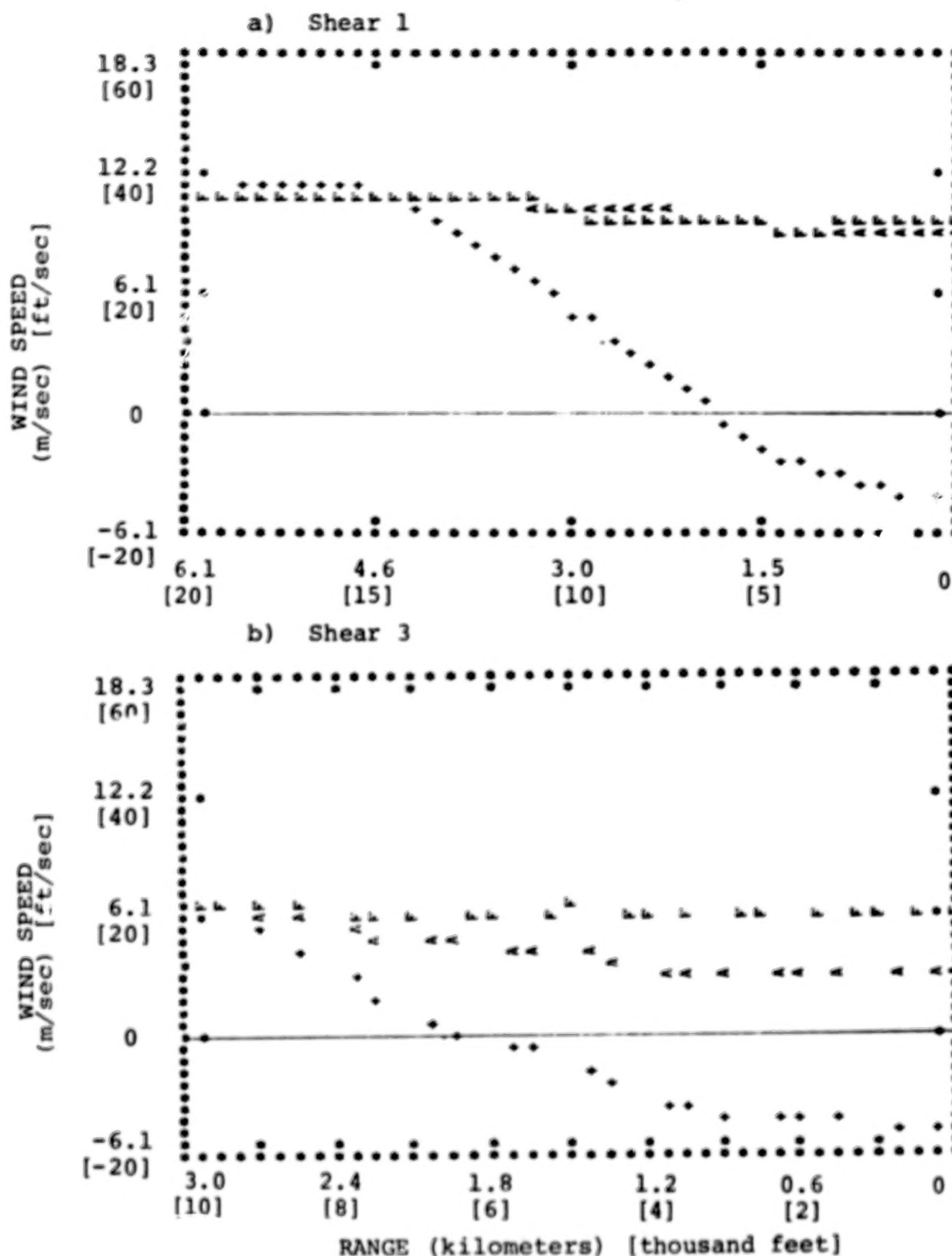


Figure 17. Effect of Display on Predicted Ability to Estimate Longitudinal Wind Component Attitude CWS.
(+) = Actual wind, A = estimate with advanced display, F = estimate with flight director.

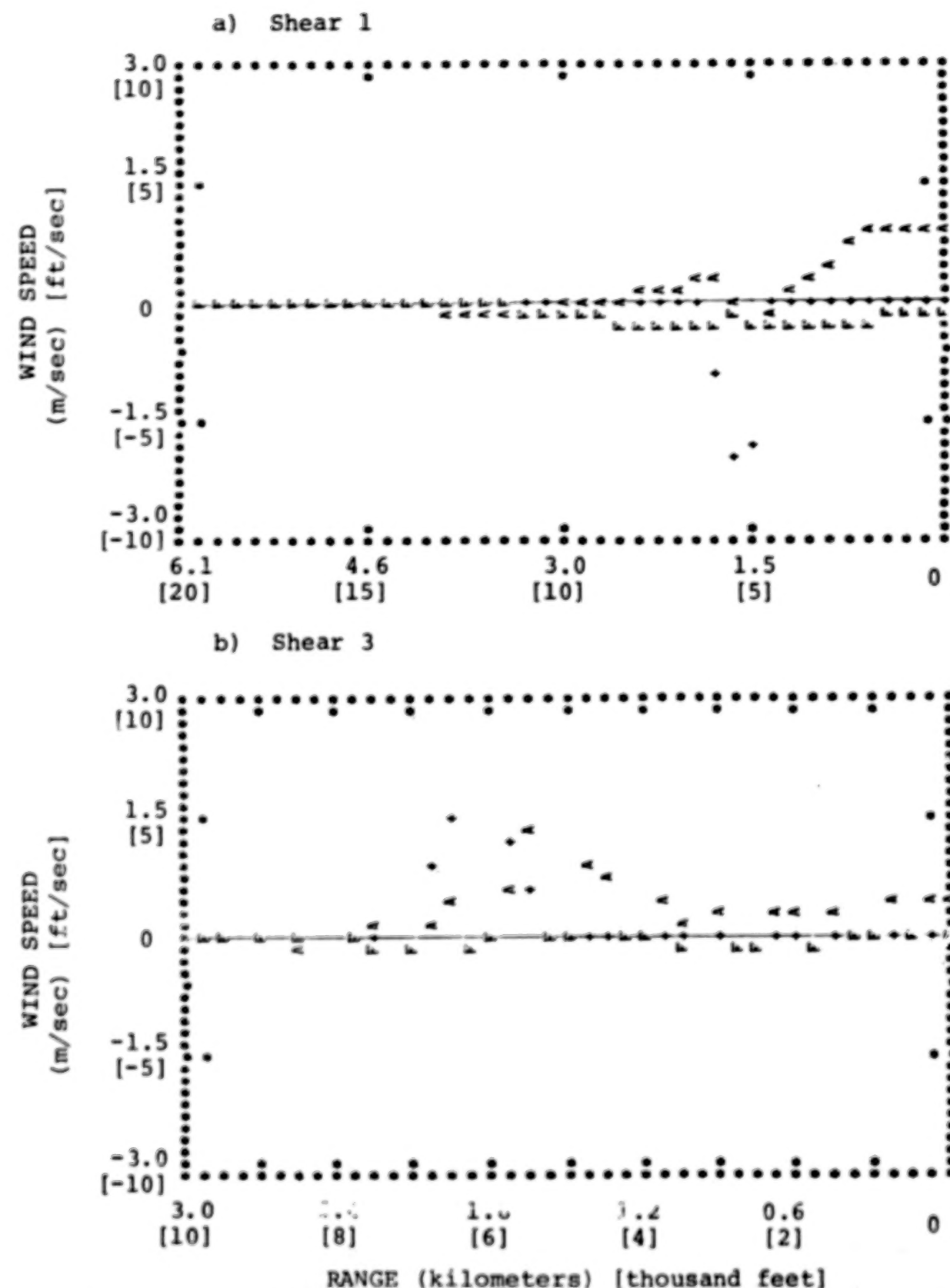


Figure 18. Effect of Display on Predicted Ability to Estimate Vertical Wind Component

Attitude CWS.

(+) = Actual wind, A = estimate with advanced display, F = estimate with flight director.

To further explore display-related differences in a moderately severe shear environment, model analysis was performed for a revised Shear 3 configuration in which the updraft was replaced by a downdraft. Comparison of Figure 19 with Figures 5 and 7 shows that the primary effect of reversing the direction of the vertical wind component is to produce a larger and more consistently negative height error. The airspeed error profile is changed relatively little. Display trends are consistent with those noted earlier: the director display leads to larger negative errors and larger predicted swings in error over the course of the approach.

To obtain an upper bound on performance improvements that could be expected from providing the pilot with better knowledge of the wind environment, performance predictions for the Shear 1 and revised Shear 3 environments were obtained for an augmented display. Specifically, the advanced display as described earlier was considered, with additional, direct, displays of horizontal and vertical wind assumed. Thresholds relating to perception of wind velocities were neglected, and an integrated display was assumed (i.e., noise/signal ratios remained at -17 dB for all display quantities. The intent here was not to simulate a physically realizable display, but to determine the performance potential associated with improved estimation of the wind environment.

Figures 20 and 21 compare predicted mean height and airspeed errors for the augmented and unaugmented advanced display. Performance with the two displays is nearly identical over most of the approach, with some tendency for the augmented display to allow tighter regulation of airspeed at the expense of slightly

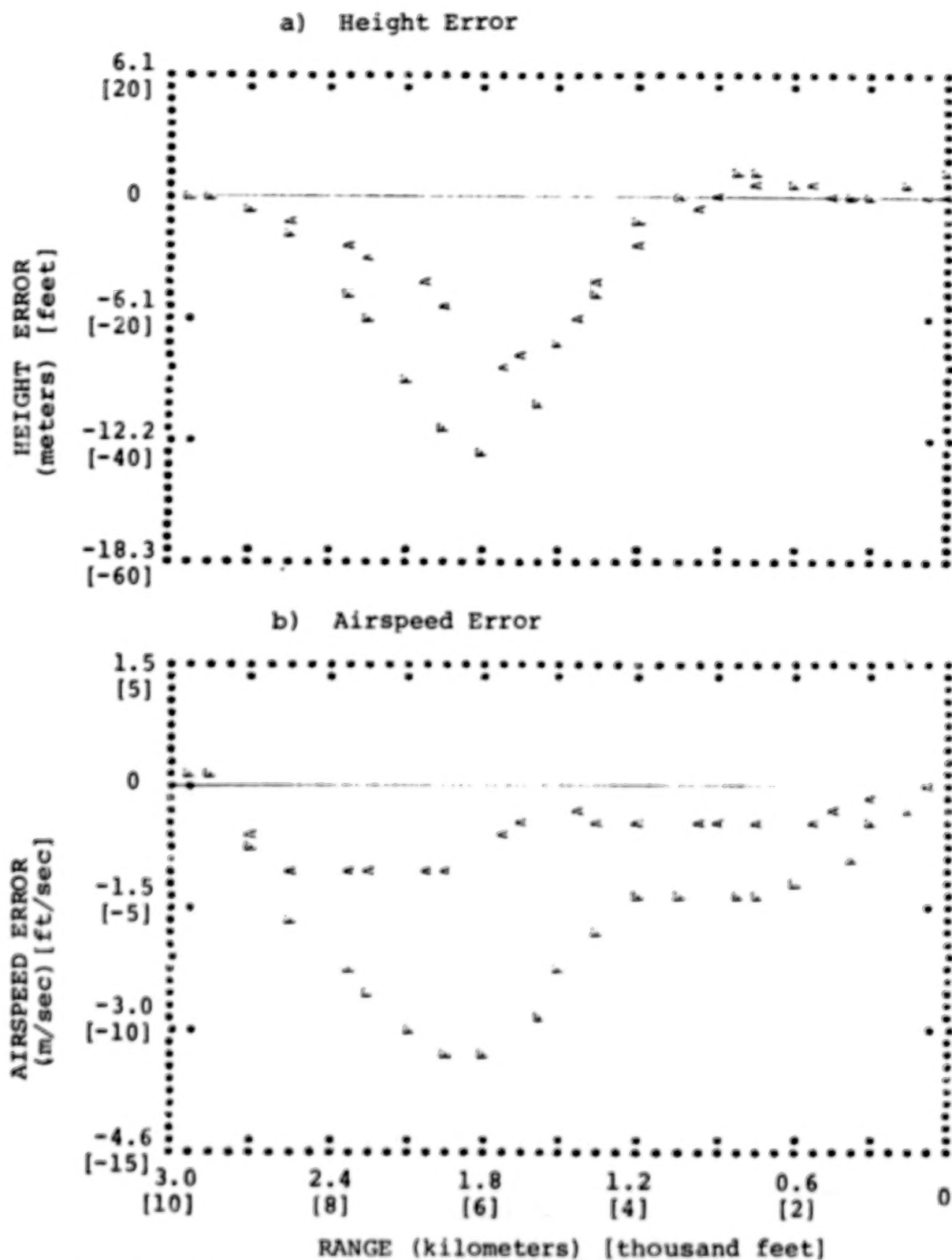


Figure 19. Effect of Display on Predicted Mean Error, Shear 3 with Downdraft

Attitude CWS.

A = advanced display, F = flight director.

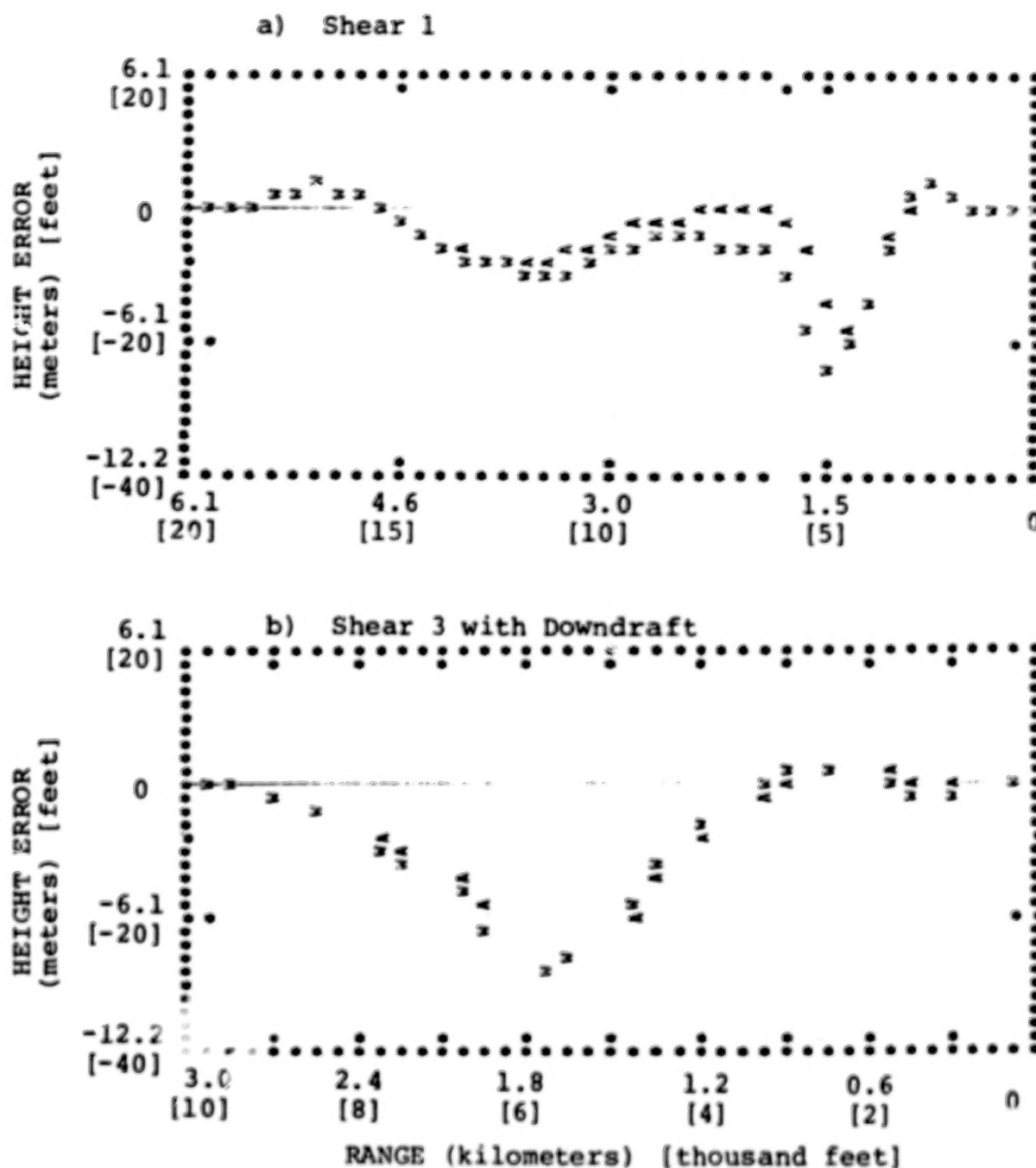


Figure 20. Effect of Explicit Display of Wind on Predicted Mean Height Error

Attitude CWS

A = advanced display, W = additional wind display

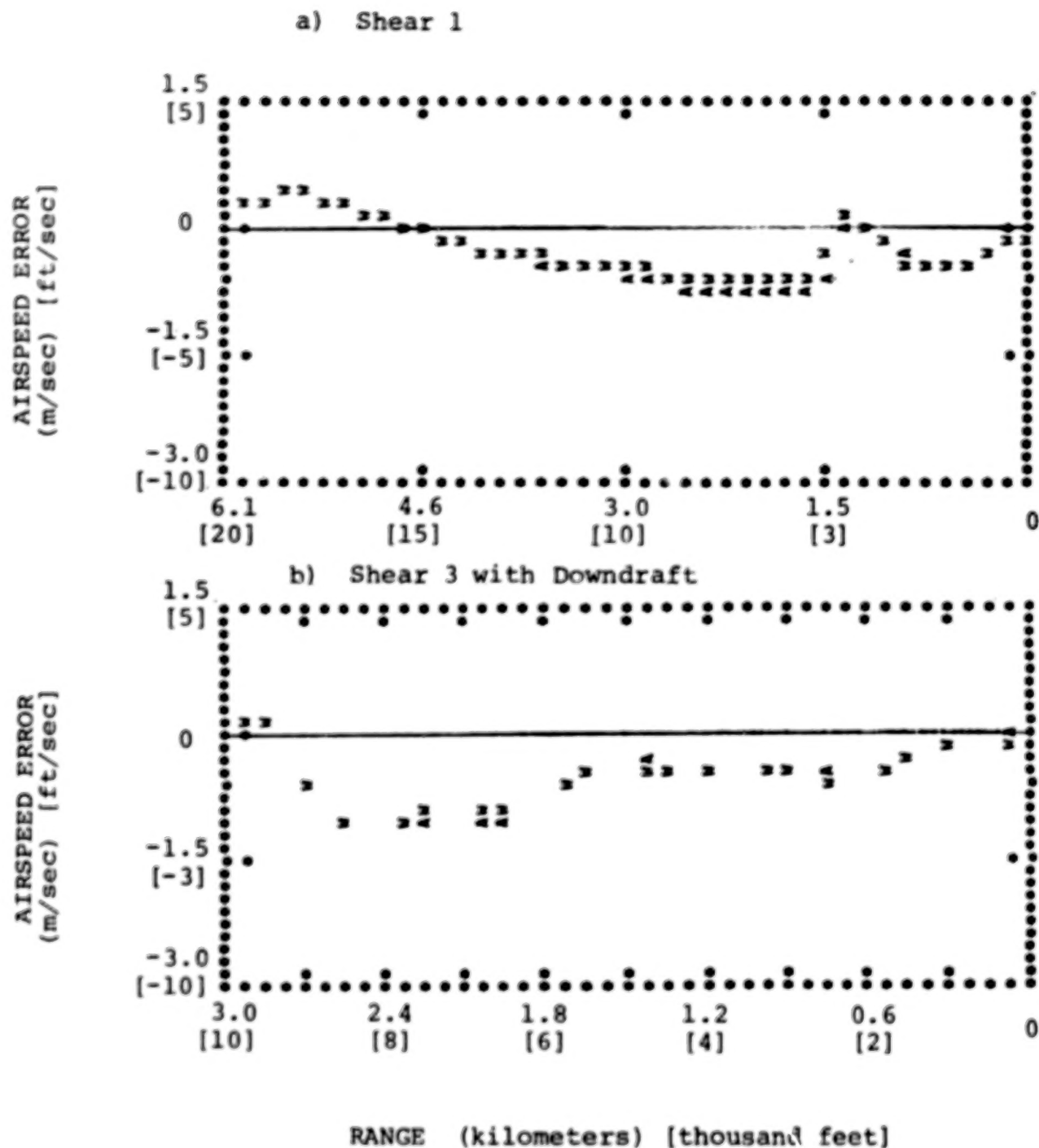


Figure 21. Effect of Explicit Display of Wind on Predicted Mean Airspeed Error
Attitude CWS.
A = advanced display, W = additional wind display.

greater height error. Thus, it would appear that little overall improvement in performance can be expected from a display which provides the pilot with improved estimates of the instantaneous wind environment.

This latest result is contingent on the assumption that the pilot does not attempt to estimate the altitude- (hence, time-) varying nature of the shear but attempts only to estimate the current wind vector. It is possible that performance could be improved if the pilot were to attempt to extrapolate the wind-- especially if the display were augmented to provide such predictive information. The potential for predictive capabilities of both pilot and display is a relevant area for future study.

4. EXPERIMENTAL STUDY

Results of the NASA-LRC TCV simulation study--as they relate to the model analysis discussed above--are presented. We first review the nature of the study, compare experimental results with model predictions, and summarize additional model analysis undertaken to match certain aspects of experimentally-observed system performance.

4.1 Description of Experiments

The aircraft simulator was configured to represent the nonlinear equations of motion of a B-737 aircraft having a weight of 40,824 kg. This simulation and a 0.3 \bar{c} center-of-gravity position was validated by both NASA and Boeing pilots.

The experimental task was to track a 3° ILS beam to touchdown. Each experimental trial began at a simulated range of 6700 m from the runway threshold at an altitude of approximately 366 m. The aircraft was initially trimmed on the desired glide path for a 3° path angle in its approach configuration: 120-knot airspeed laps, gear down. Rudder was automatically controlled.

Zero-mean random gusts and wind shears were both simulated during each experimental trial. The simulated shear was generated as described above in Section 2.3. Three shear environments were explored, including those designated as "Shear 1" and "Shear 3", profiles of which are given in Figure 3.

Gust disturbances having an rms variation of 0.3m/sec were simulated for all three translational axes. Gust spectral characteristics were varied with altitude according to the wind models suggested by Chalk et al. [2].

Data were obtained from three NASA test pilots. Practice trials were provided using shears other than those specified for data collection. Each pilot "flew" two sessions of 18 approaches each for data collection; each session consisted of two replications of 3 control/display configurations and 3 shear environments presented in a balanced order. Thus, four replications per experimental condition per pilot were obtained.

The size of the data base reflects a compromise between the need for reliable statistics and the requirement to minimize learning. To obtain reliable estimates of ensemble mean and standard deviation, a minimum of 10 trials/subject/condition would have been desired. However, we anticipated that the test pilots would begin to learn the specific shear profiles if given this degree of exposure, in which case the experimental task would be of little operational significance. Hence, the compromise of four replications per subject/condition was adopted.

Table 4 shows the number of trials analyzed per subject for each experimental condition. (Only data from two of the three shear environments explored experimentally are relevant to this analytical study.) Note that data were not obtained for the flight director, velocity CWS configuration.

4.2 Data Analysis Procedures

Ensemble statistics were computed for selected response variables for each experimental condition. First, within-subject replications were analyzed to provide trajectories of mean response and of the standard deviation of the response. The standard

Table 4

Data Base

Shear	Pilot	Control/Display Configuration		
		Attitude CWS Flight Director	Attitude CWS Advanced Disp	Velocity CWS Advanced Disp
1	G	3	3	3
	J	4	4	4
	Y	4	4	4
3	G	3	3	3
	J	2	2	2
	Y	4	4	4

Entries indicate number of trials/subject/condition available for analysis.

deviation obtained at this stage of the analysis indicates inter-trial differences and reflects the effects of stochastic aspects of the flight task (i.e., random turbulence and within-pilot response variability.) These measures were processed further to provide across-subject averages of the mean and standard-deviation response trajectories. Mathematical definitions of these statistical variables are given in Levison and Baron.

For purposes of data presentation in this report, statistical analysis was performed for height and airspeed errors, sampled at 305 meter intervals beginning at a range of 4572 m from the ILS origin.*

4.3 Comparison of Predicted and Experimental Results

Let us now compare the trends of display and control effects observed experimentally with trends predicted by the model. We note that the model results presented here and in the preceding section are true predictions; pilot-related model parameters were selected on the basis of previous results or by assumption (the latter being the case for newly-introduced parameters related to treatment of nonrandom inputs. No attempt was made at this stage to match model results to data.

Because of the various sources of uncertainty in both experimental results as well as model prediction, one should look mainly for confirmation of trends rather than for

*Unlike the analysis performed in the preceding phase of this study, no within-trial averaging (i.e., data smoothing) was conducted.

accurate numerical correlation between predictions and data. We have already noted the need to assume values for newly-introduced model parameters in the absence of previous experimental validation, as well as the smallness of the data base necessitated by the desire to minimize the subjects' learning of the windshear profile. Furthermore, inspection of the results of individual trials reveals the presence of inconsistent biases in control strategy. - For example, one of the test subjects tended to carry excess airspeed for some of the experimental trials but not for other trials. Thus, the most reliable trend to look for is the variation in error along the course of the approach.

The next eight figures compare display and control trends for predicted and experimental mean response trajectories for the two shear environments explored in this analysis. Because the experiment was not full factorial, display differences are shown for the Attitude CWS configuration only, and control differences are compared for the advanced display configuration.

Display effects are compared in Figures 22 through 25. In general, the trends predicted by the model are confirmed, but the differences observed experimentally are smaller than predicted. Model and experimental correlation is generally better for height than for speed response.

Figures 22 and 23 show that, as predicted, experimental height error is generally more negative for the director than for the advanced display. The data also confirm the prediction that the director display leads to a larger swing in error over the course of the approach in the Shear 1 environment (Figure 22) but not in the Shear 3 environment (Figure 23). Both figures show a tendency (not predicted) for the pilots to fly above the nominal glide path.

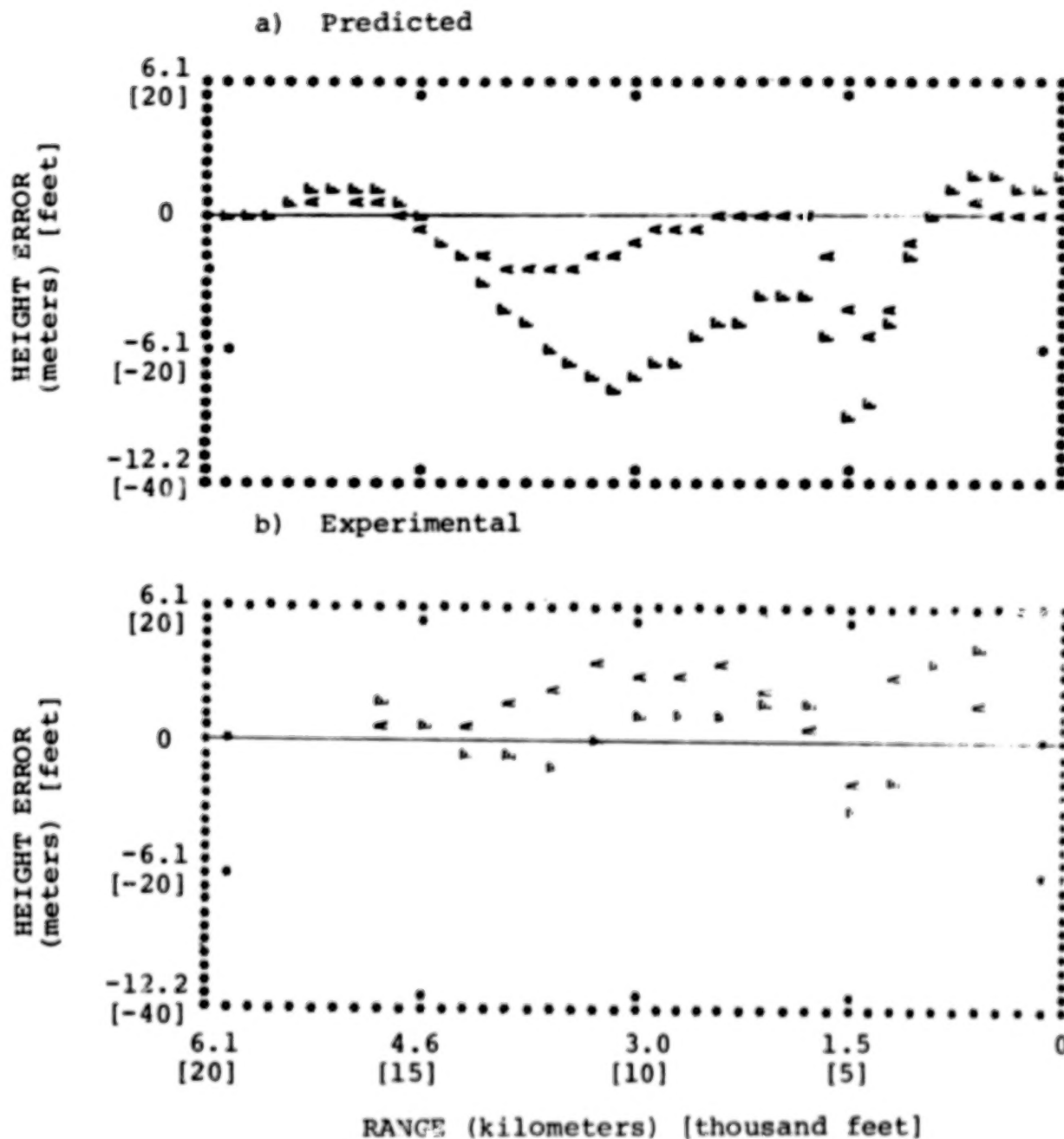


Figure 22. Effect of Display on Mean Height Error, Shear 1 Attitude CWS.
A = advanced display, F = flight director.

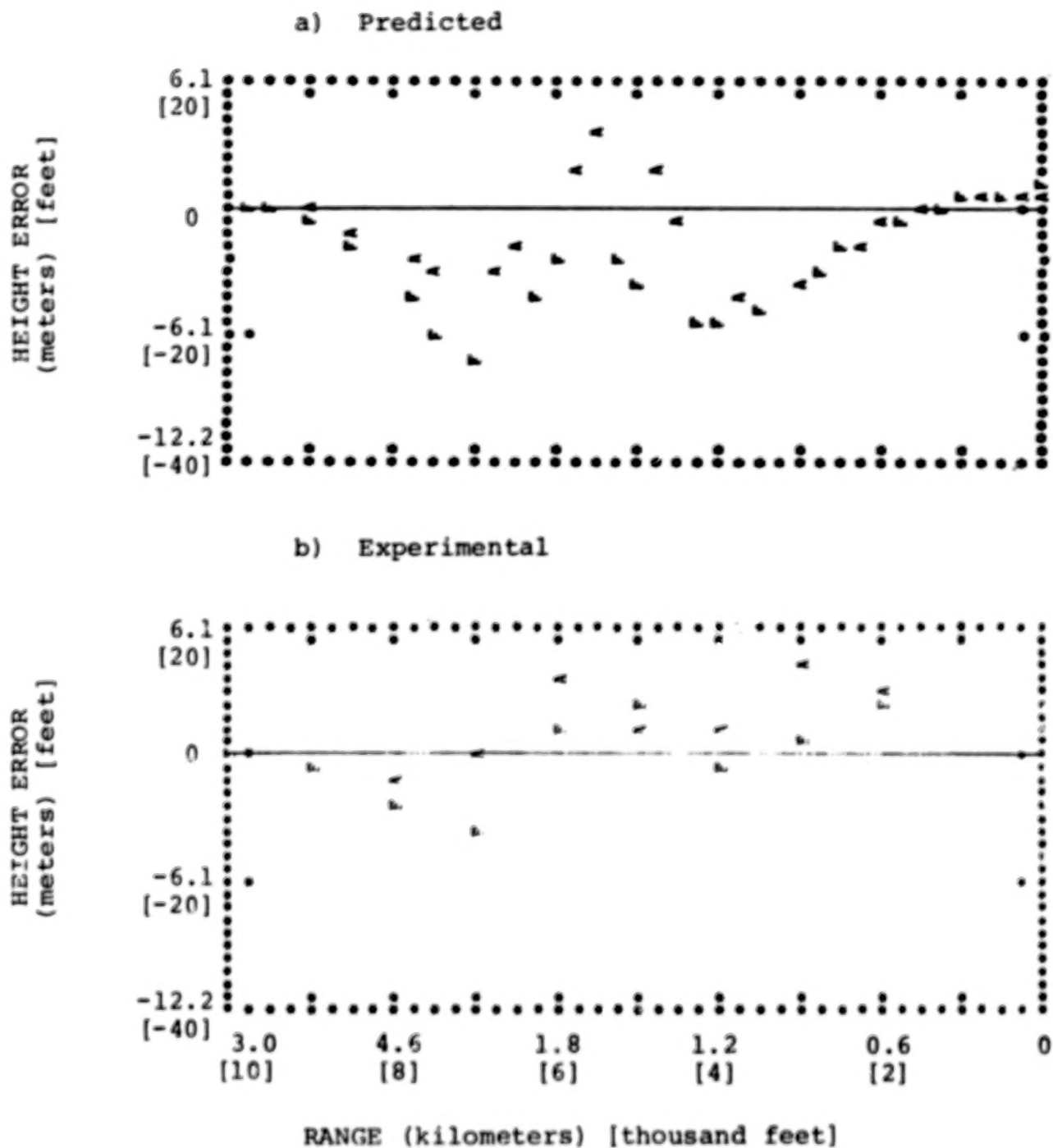
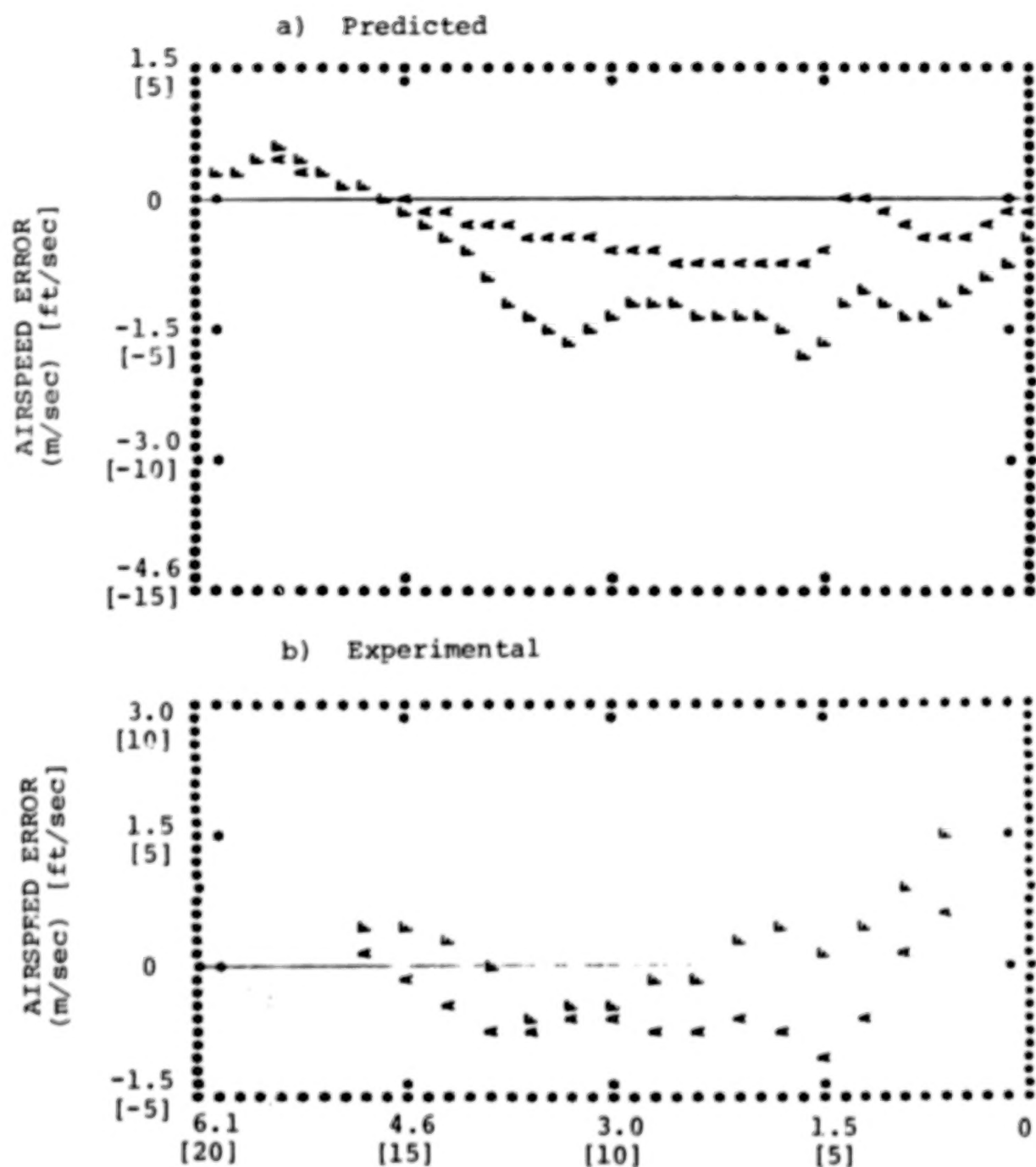


Figure 23. Effect of Display on Mean Height Error, Shear 3

Attitude CWS.

A = advanced display, F = flight director.



RANGE (kilometers) [thousand feet]

Figure 24. Effect of Display on Mean Airspeed Error, Shear 1

Attitude CWS.

A = advanced display, F = flight director

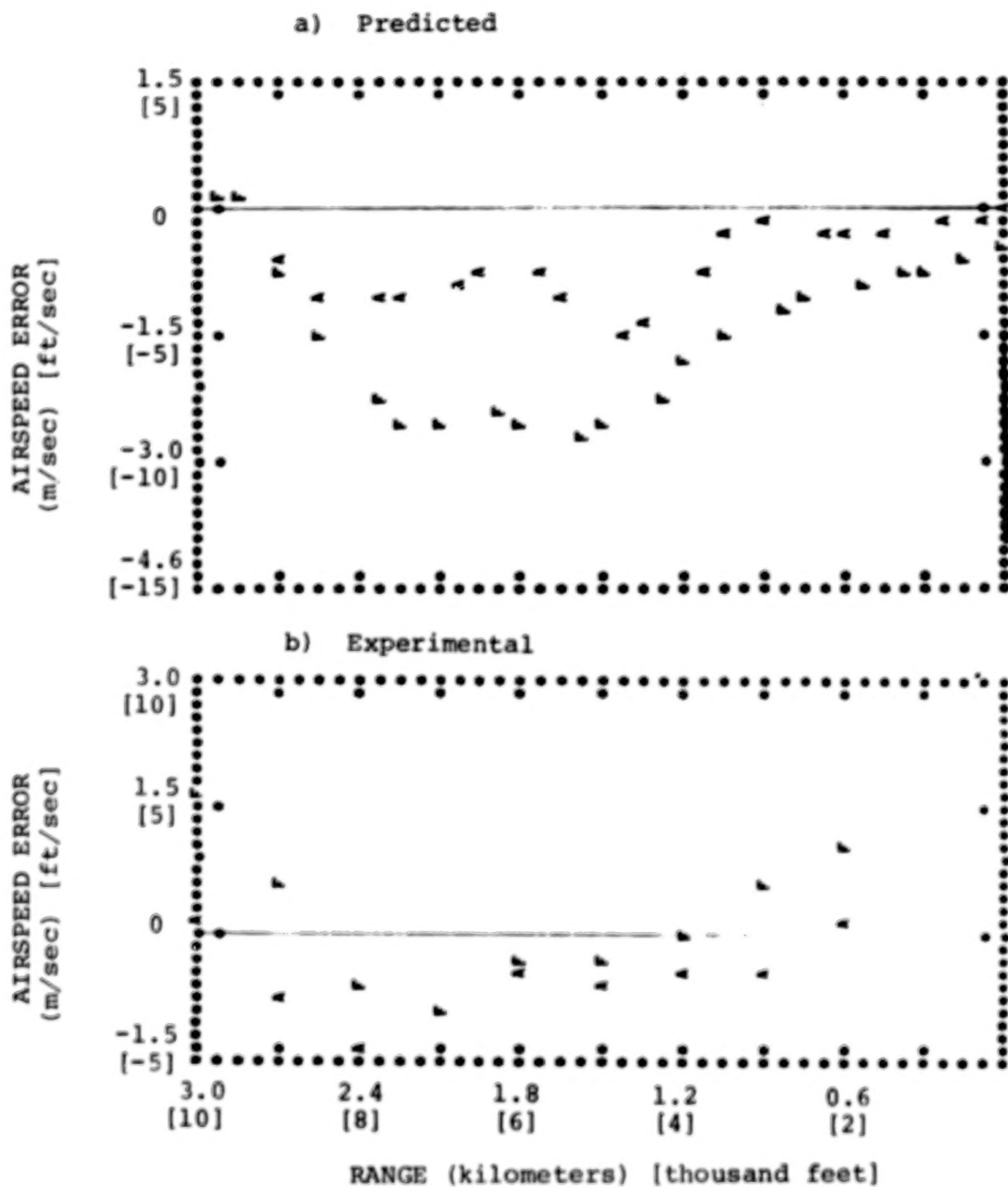


Figure 25. Effect of Display on Mean Airspeed Error, Shear 3

Attitude CWS.

A = advanced display, F = flight director

Figures 24 and 25 show that the test pilots flew the director display with less negative (or more positive) airspeed errors than achieved for the advanced display--a trend the reverse of which was predicted by the model. Given the reported tendency of pilots to fly approach speeds greater than nominal when windshears are anticipated (3), we suspect that the test subjects attempted to compensate for the lack of good airspeed information from the director configuration by intentionally carrying excess airspeed. Experimental results confirm the prediction of greater swings in error with the director display, although the magnitudes of the display-related differences are less than predicted.

Figures 26 through 29 confirm the major trends predicted for control effects; namely, tighter regulation of height error is observed for velocity CWS, whereas control configuration has little effect on regulation of speed error.

Mean profiles, along with respective 1-sigma envelopes, are shown for height and airspeed errors, respectively, in Figures 30 and 31. Comparison with Figures 12 & 13 reveal that experimental standard deviations were from 2 to 3 times as great as those predicted by the model. To some extent, the larger response variability found experimentally may have been due in part to changes in the pilot's subjective reference point from run-to-run. In addition, it is possible that one or more of the assumptions and simplifications adopted for the model analysis introduced errors in predicted response behavior. Sensitivity analysis to some of the modelling aspects is presented below in an attempt to provide a better match between predicted and measured behavior.

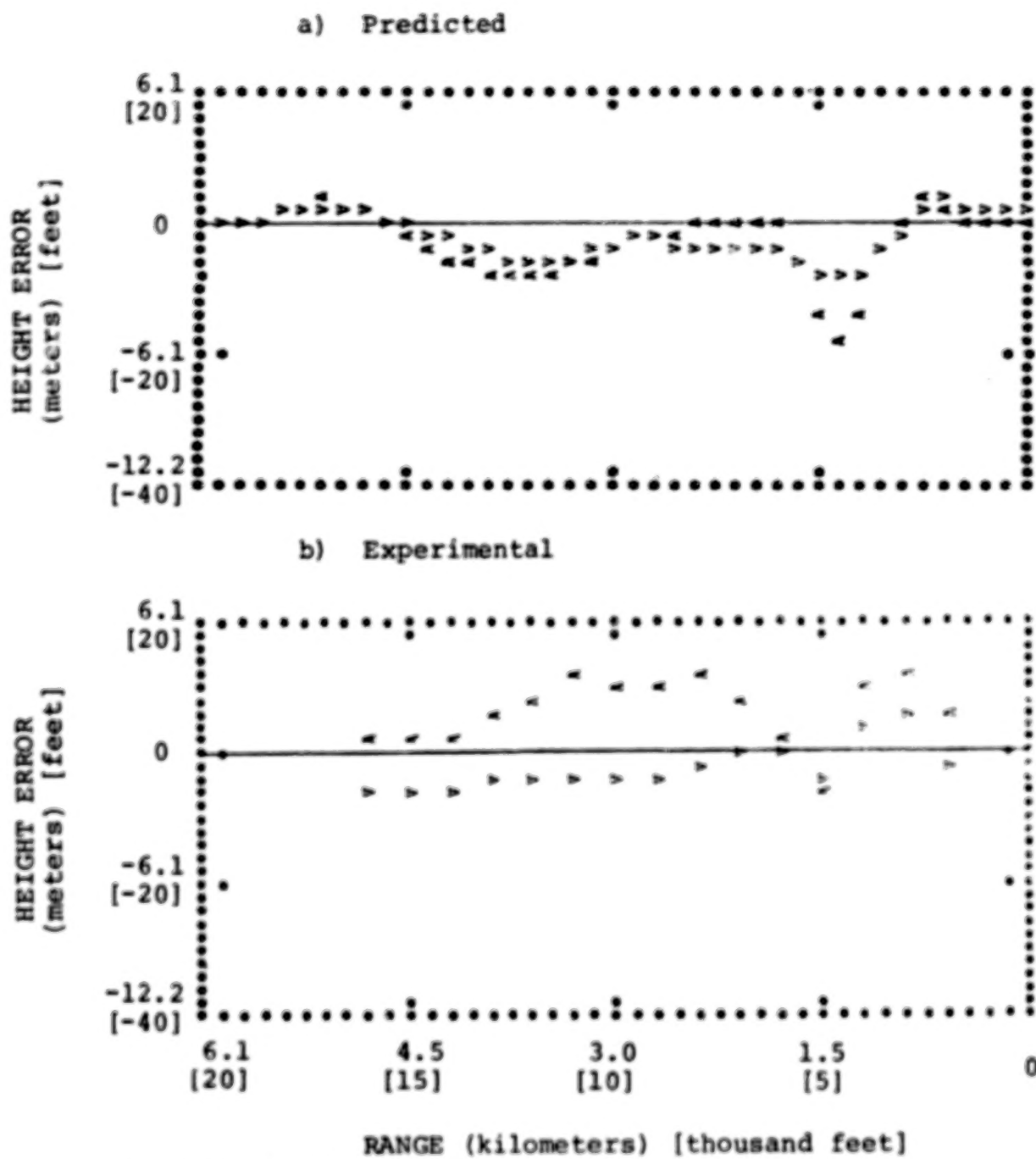


Figure 26. Effect of CWS on Mean Height Error,
Shear 1

Advanced Display.

A = attitude CWS, V = velocity CWS.

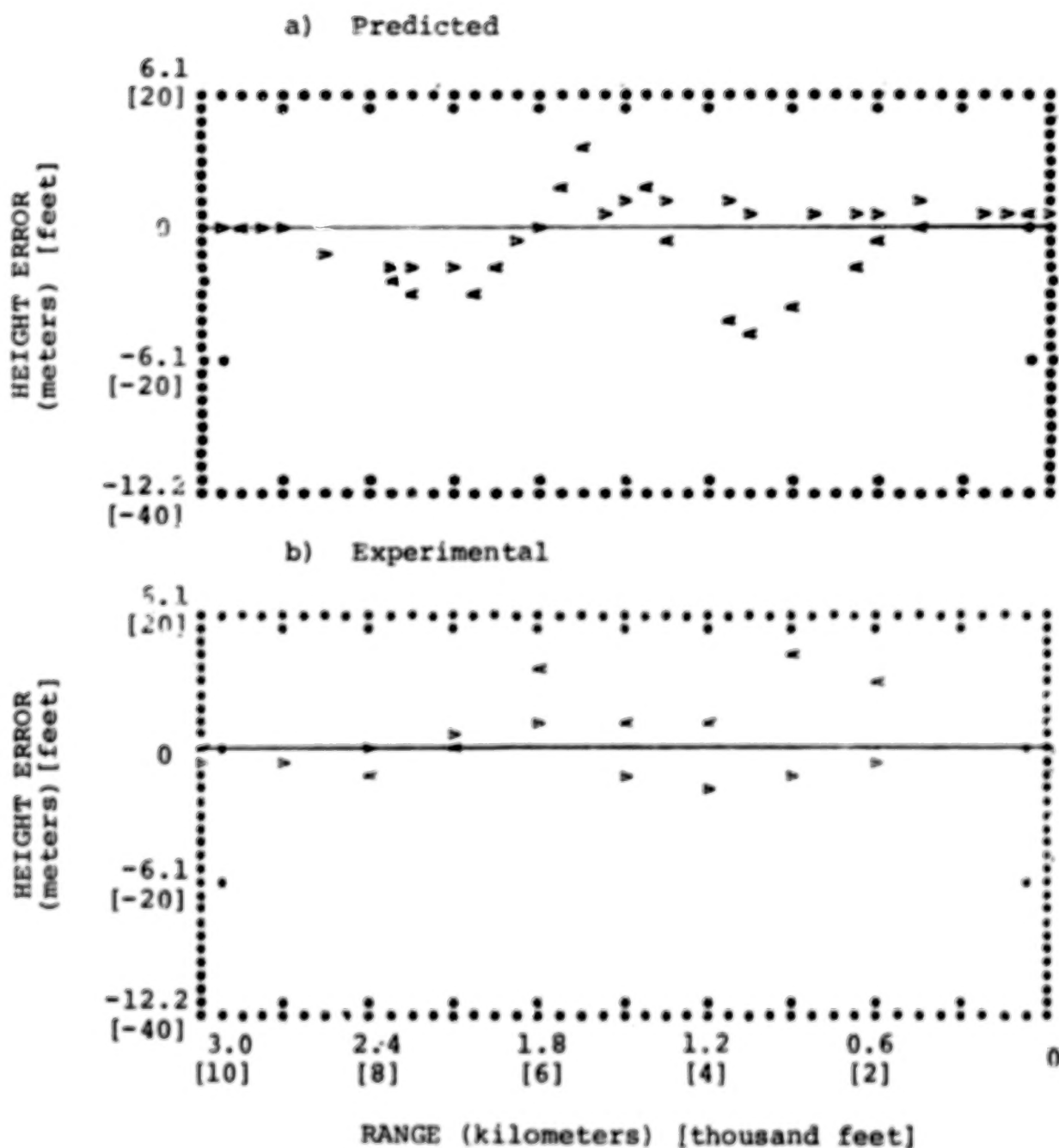


Figure 27. Effect of CWS on Mean Height Error, Shear 3

Advanced display.

A = attitude CWS, V = velocity CWS.

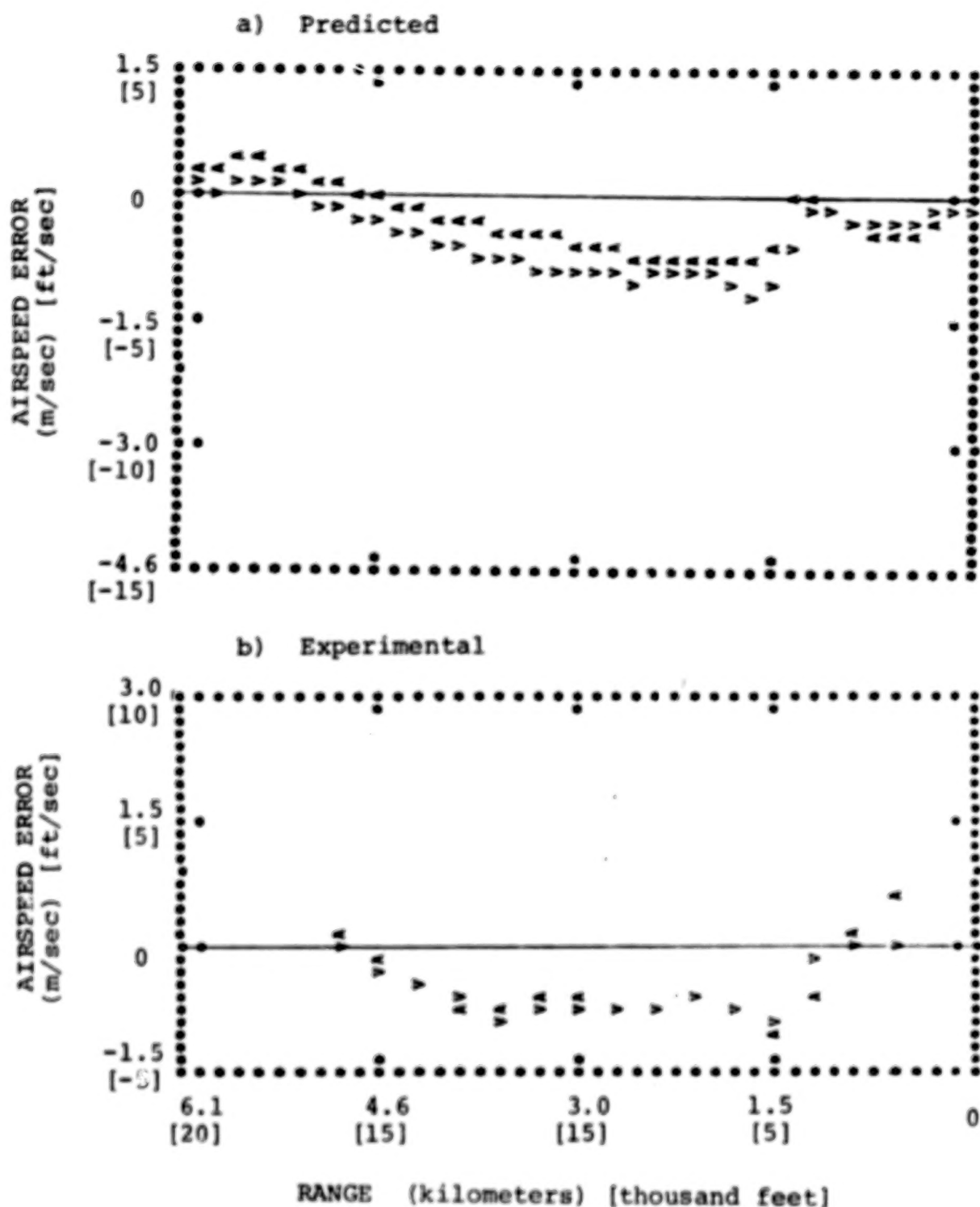


Figure 28. Effect of CWS on Mean Airspeed Error, Shear 1
Advanced display.
A = attitude CWS V - velocity CWS

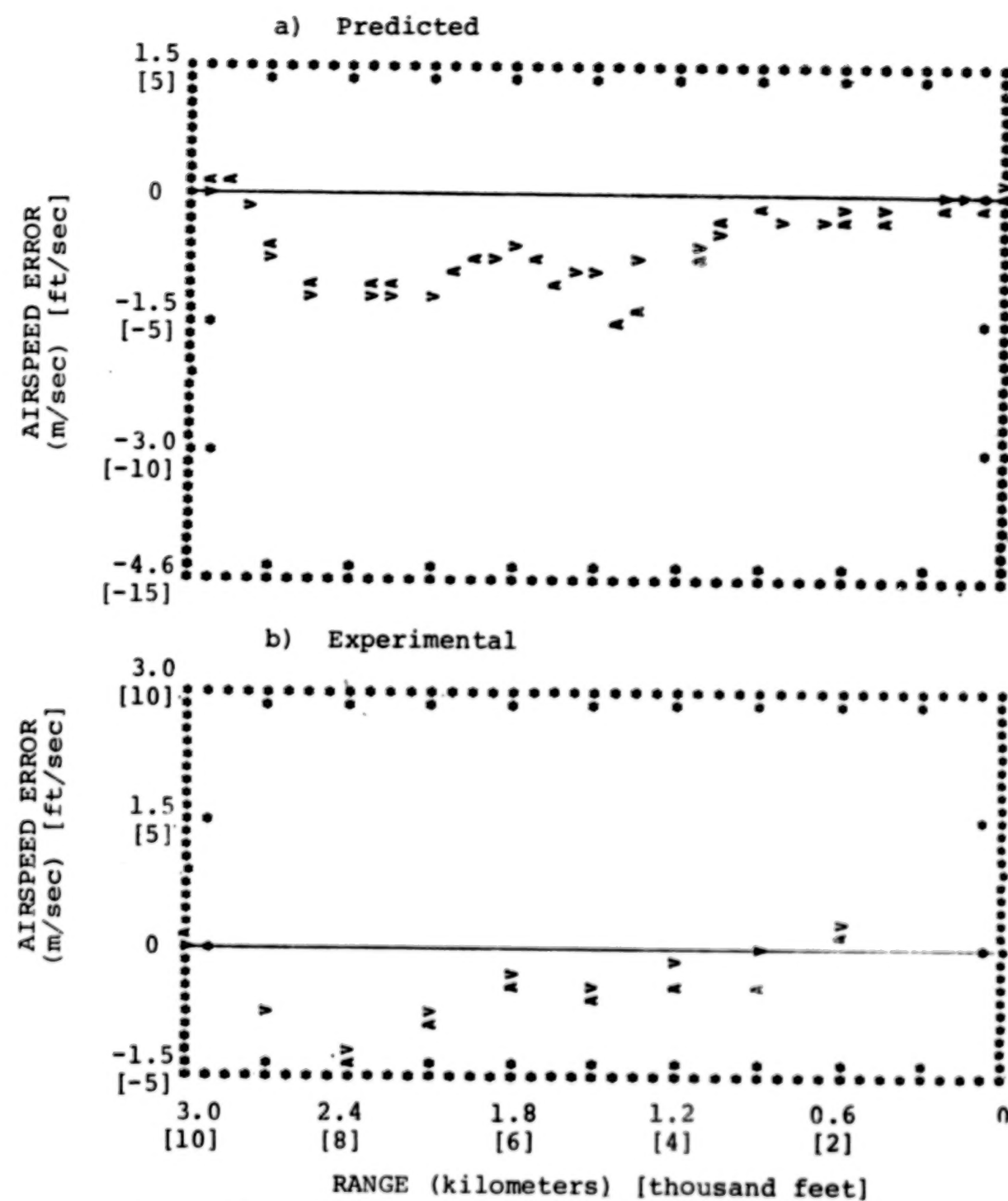


Figure 29. Effect of CWS on Mean Airspeed Error, Shear 3 Advanced display.
A = attitude CWS, V = velocity CWS.

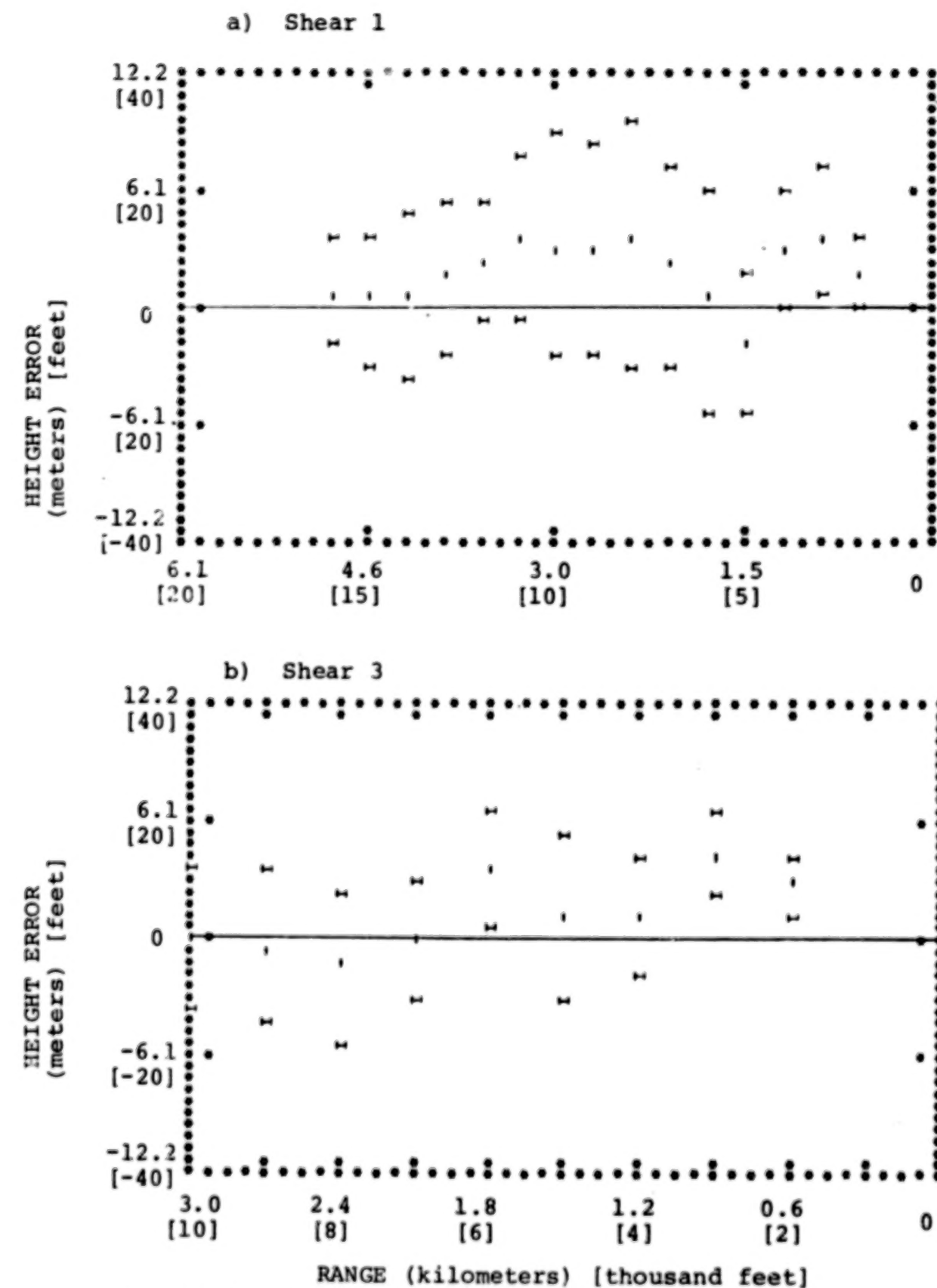


Figure 30. Mean and Standard Deviation of Experimental Height Error
Advanced Display, Attitude CWS

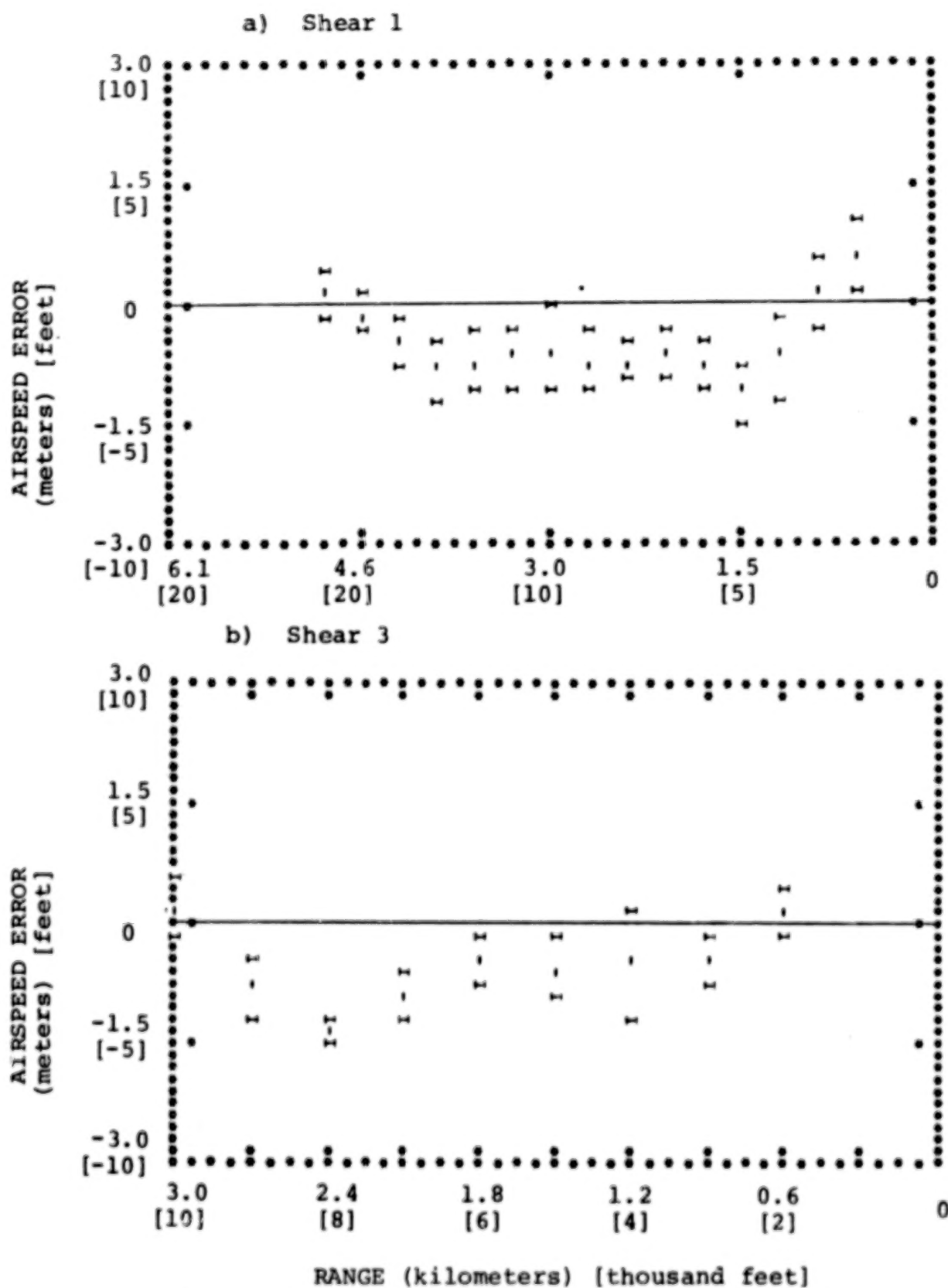


Figure 31. Mean and Standard Deviation of Experimental
Airspeed Error

Advanced display, attitude CWS.

4.4 Post-Experimental Model Analysis

Although the trends of control- and display-related performance differences were, in general, predicted correctly by the model, the differences observed in the simulation experiments tended to be smaller than predicted. Also, response variability was from two to three times as great as predicted.

Various assumptions and simplifications were necessary to define the problem for model analysis. Some of the factors that could have been responsible for predictive inaccuracies are considered below.

The magnitude of the display-related differences predicted by the model is a function of the perceptual thresholds associated with informational quantities provided by the two displays. Quite possibly, the assumption of a 2-knot indifference threshold on airspeed as obtained from the panel indicator (associated with the flight director configuration) was pessimistic. To test the importance of this assumption, the director configuration was reanalyzed with a threshold of 0.825 knots (0.427 m/sec) associated with airspeed perception as computed on the basis of visual resolution limitations (see Baron and Levison [1]).

Mean height and airspeed errors predicted for the director display with reduced airspeed threshold are compared with predictions obtained for the advanced display in Figure 32. (Shear 3 environment). Comparison with previous model predictions (Figures 5 and 7) and with experimental results (Figures 23 and 25) shows that the reduced airspeed threshold decreases the performance differences and, therefore, brings the model predictions into greater correspondence with display-related differences observed experimentally. The change in

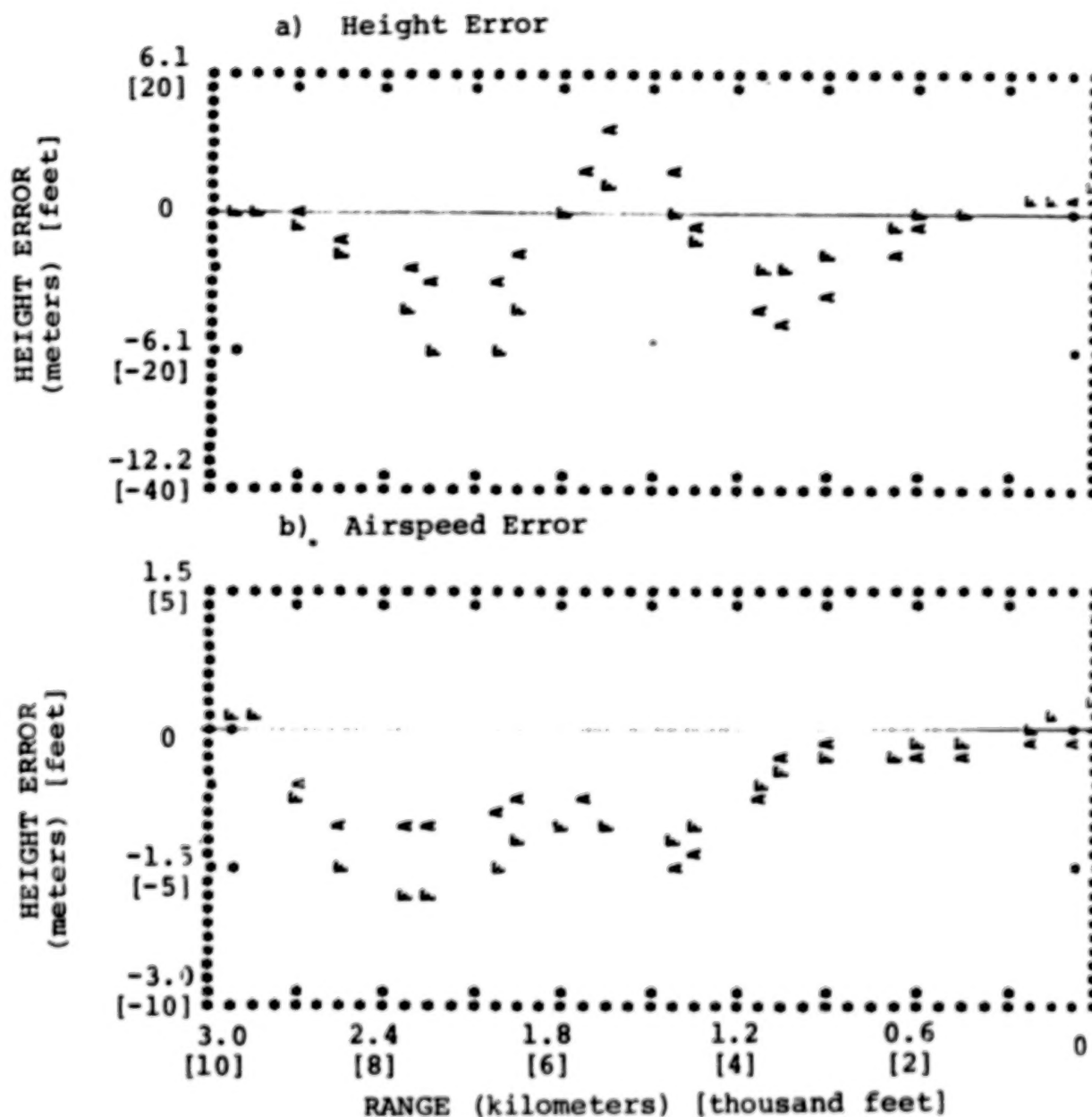


Figure 32. Effect of Display on Predicted Mean Error,
Low Threshold for Airspeed Perception

Attitude CWS, Shear 3

A = advanced display, F = flight director

threshold does not, of course, account for the difference between predicted and observed response variability.

There are a number of potential causes for the underestimation of response variability. We have already noted the apparent tendency of the pilots to adopt different reference levels of height and airspeed on different experimental trials. Other possible sources of error include (1) underestimation of pilot observation noise/signal ratio, (2) underestimation of the degree of pilot uncertainty associated with the detection and response to windshears, and (3) underestimation of other sources of response variability.

To explore the effects of increased noise/signal ratio (equivalently, decreased attention to the task) on the predicted response behavior, the Shear 3, attitude CWS, task was reanalyzed with noise/signal ratios increased by 6 dB. Comparison of the response envelopes shown in Figure 33 with corresponding trajectories of Figures 12b and 13b show that increased noise did, on balance, increase response variability for the advanced display configuration (although not nearly to the level observed experimentally). A similar trend is predicted for the flight director display (not shown). Figure 34, however, shows that increased noise/signal ratio increases display related mean errors (compare with Figures 5a and 7a), thereby adding to modeling error in this respect. Thus, it does not appear that alternative assumptions regarding pilot attentional levels will improve model accuracy in both mean response and response variability.

Pilot uncertainty related to the nonrandom input was manipulated in an attempt to improve the match to experimental results. A scale factor of 10 was added to the increment in

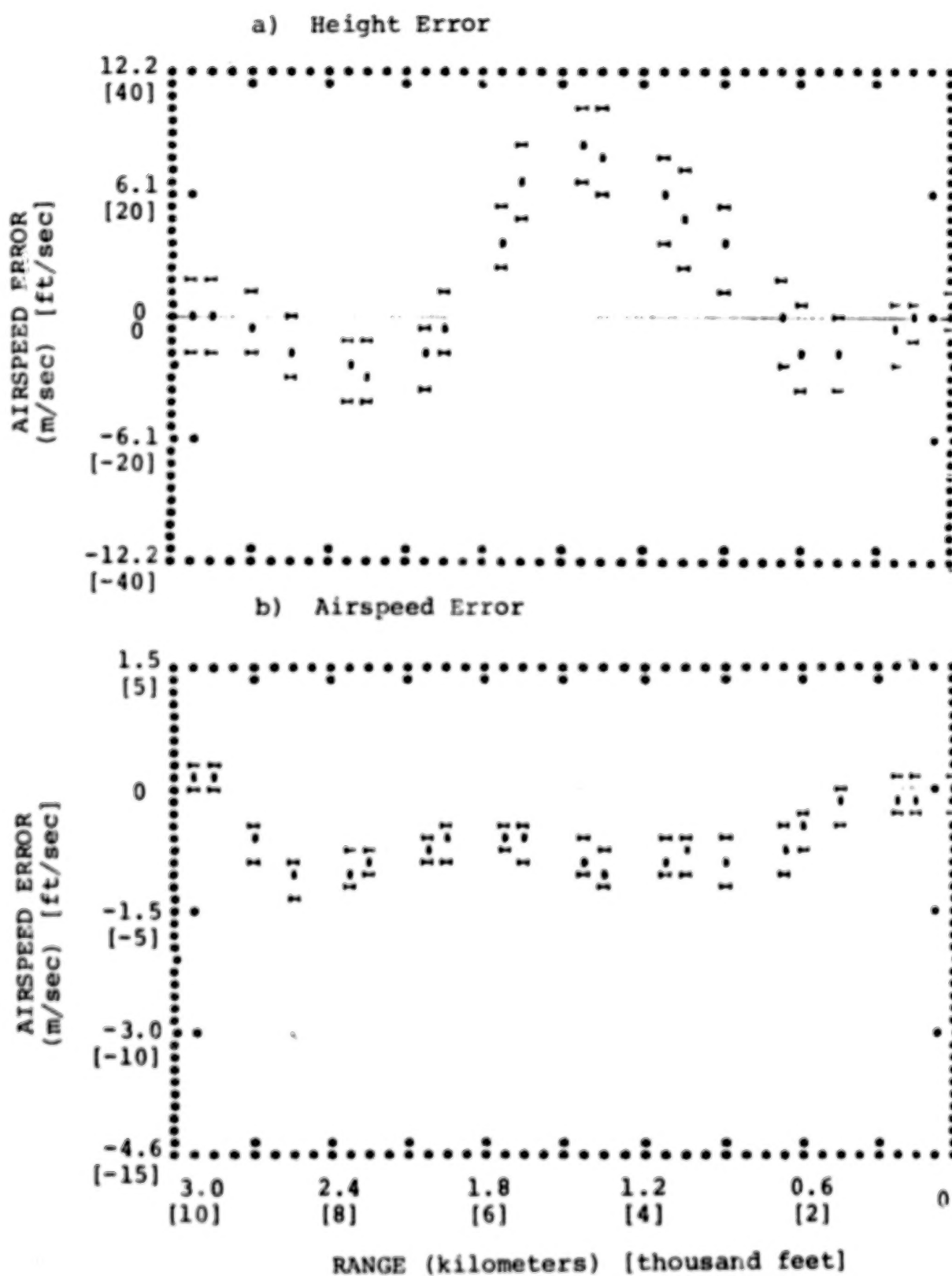


Figure 33. Predicted Response Variability for Increased Noise/Signal Ratio
Advanced Display, Attitude CWS, Shear 3

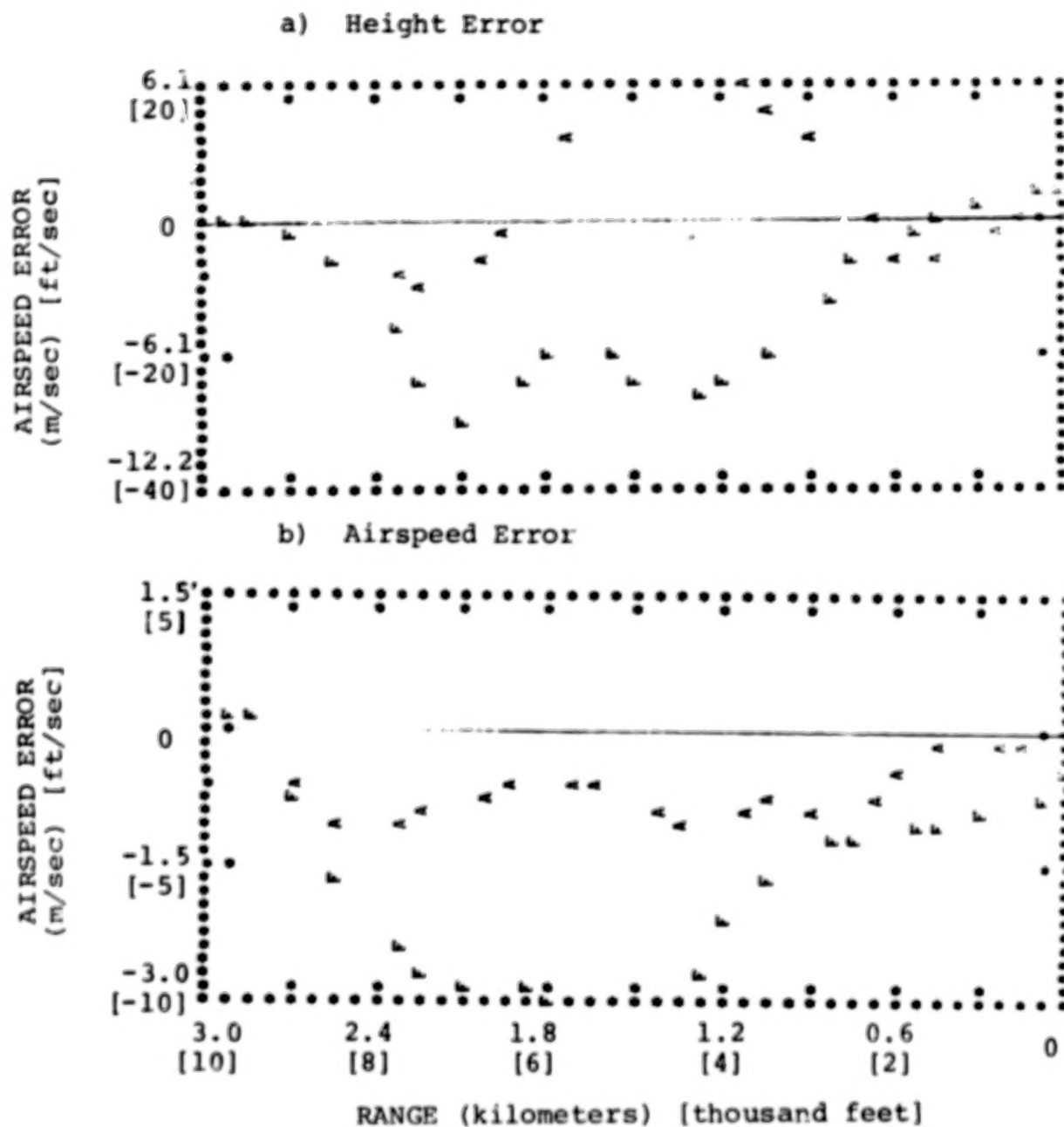


Figure 34. Effect of Display on Predicted Mean Error,
Increased Noise/Signal Ratio

Attitude CWS, Shear 3

A = advanced display, F = flight director

estimation error covariance in order to enhance the effect on performance of the pilot's detection of a nonrandom input.*

Comparison of the trajectories in Figure 35 with corresponding curves in Figures 12b and 13b reveals a slight increase in response variability associated with height error and negligible change in speed error response variability. Comparison of the mean trajectories of Figure 36 with previous model predictions shows an inconsistent effect on display-related differences. The effect of displays on mean height error is reduced - a trend, in general, that would tend to improve correspondence with experimental data. On the other hand, this scale factor has negligible effect on display-related differences in mean airspeed error. Furthermore, predicted errors tend to be relatively flat and close to zero for the final 900-1200 meters of flight - a trend not confirmed by the experimental results shown in Figure 23 and 25. The model predictions are little changed if the scaling on uncertainty is increased by another factor of 10 (i.e., overall gain of 100). Thus, modeling errors are not attributable to this particular model parameter.

Finally, model results were obtained for the Shear 3, attitude CWS task with the driving noise covariances increased by a factor of 4. This was done partly to consider the possibility that the simplified treatment of wind gusts provided a less severe disturbance than that provided in the manned simulation, and partly to simulate the presence of additional sources of variability (such as the apparent tendency of pilots

* The mathematical treatment of nonrandom inputs is summarized in the appendix.

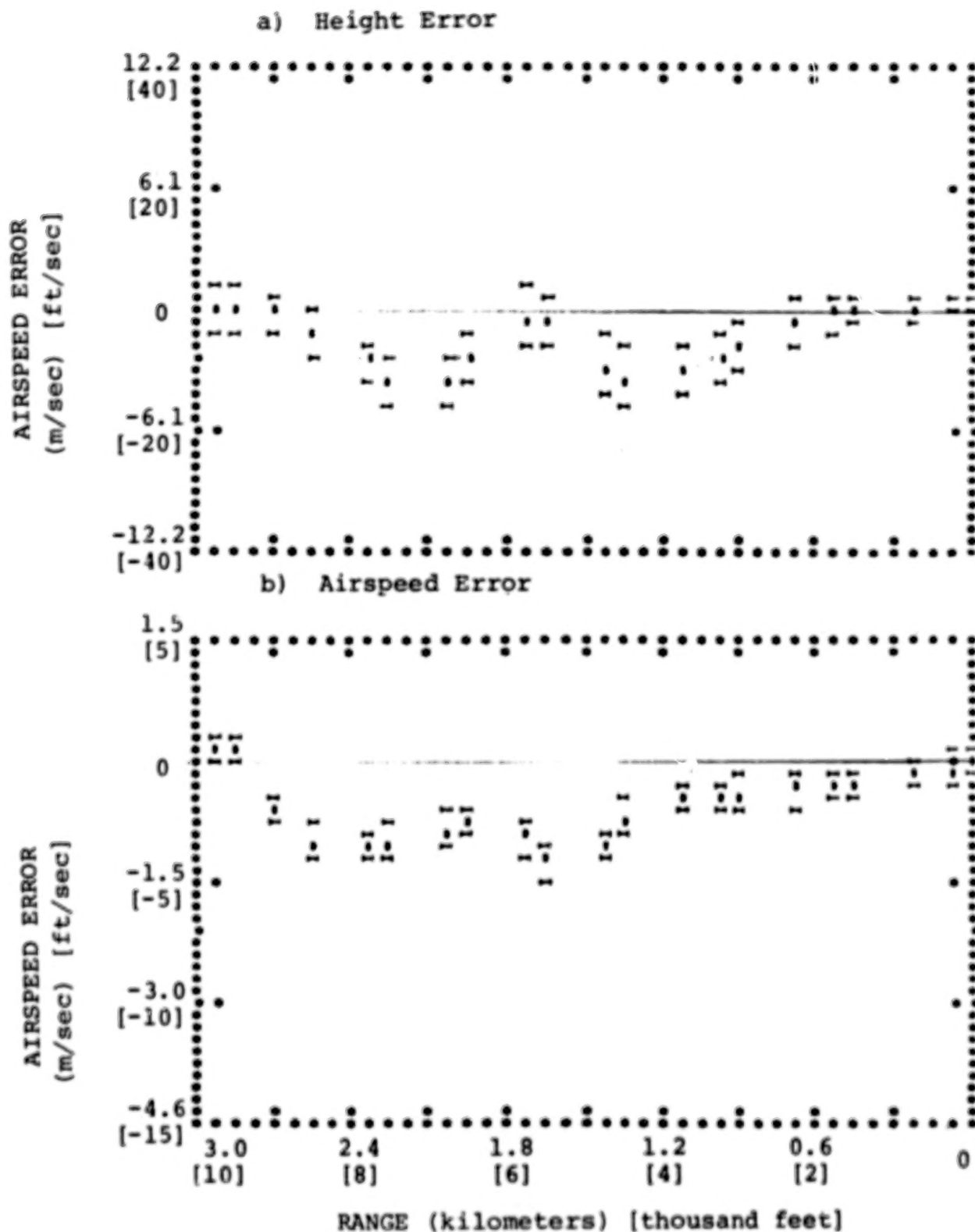


Figure 35. Predicted Response Variability for Increased Pilot Uncertainty
Attitude CWS, Advanced Display, Shear 3

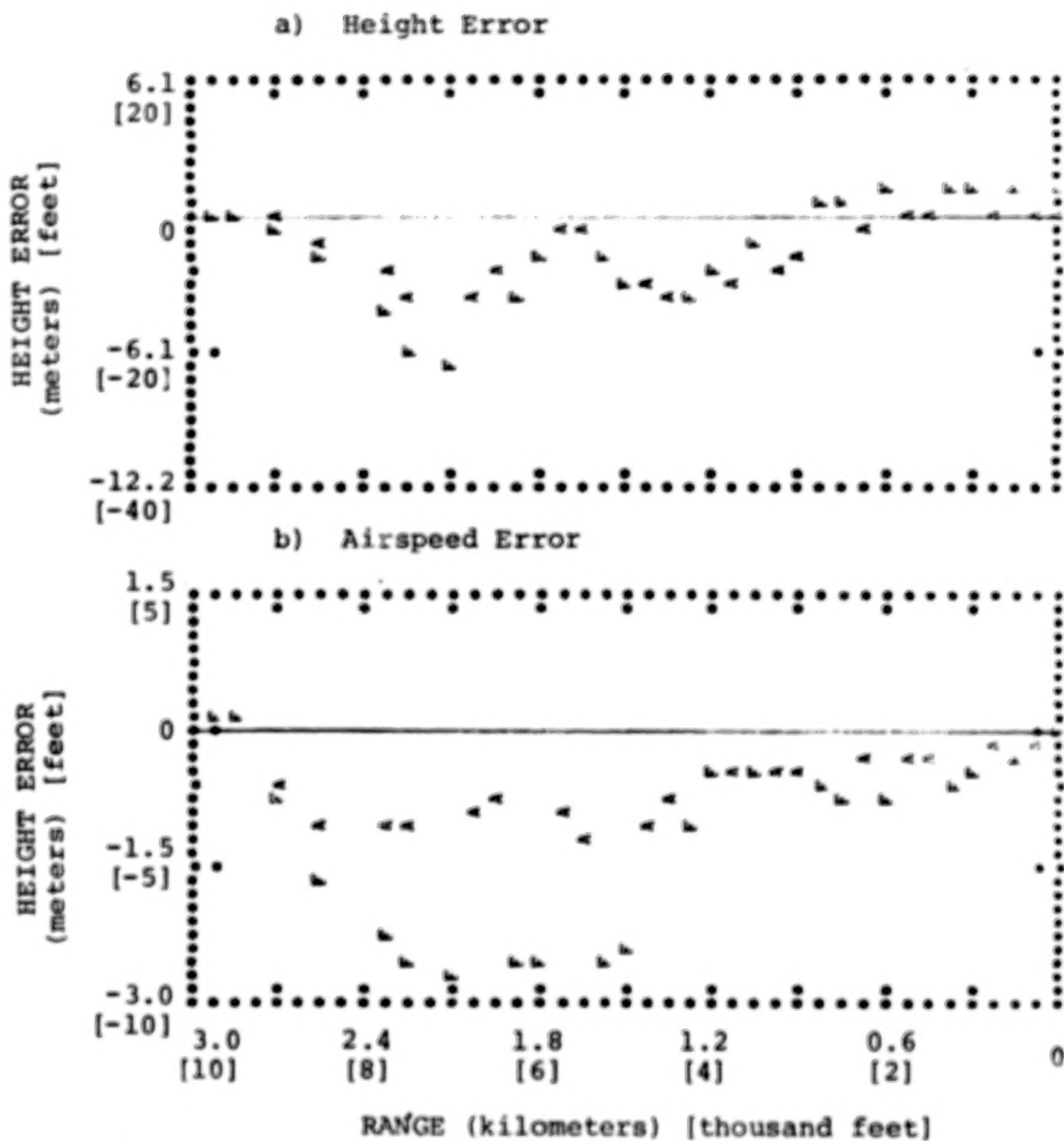


Figure 36. Effect of Display on Mean Response for Increased Pilot Uncertainty

Attitude CWS, Shear 3

A = advanced display, F = flight director

to change criteria from run-to-run). It was clear beforehand that increasing the driving noise would increase response variability; the primary result of interest was the effect of increased disturbance on mean response trajectories.

Figure 37 shows that both height and airspeed response variability increased substantially compared to previous model predictions. Furthermore, Figure 38 (compared with previous predictions) show reductions in display-related differences-- a trend that, in general, would tend to improve predictive accuracy. In terms of model behavior, the most likely explanation for the reduction in display-related differences in mean error (especially for airspeed error) lies in the fact that increased response variability increases the fraction of time that display quantities are above perceptual threshold levels, thereby reducing the effects of thresholds on performance. Since display-related differences appear to be caused primarily by threshold differences, such performance differences are reduced in the presence of greater variability.

To summarize this section on post-experimental analysis, the effects of certain model parameters on predictive accuracy have been explored. It appears that prediction of display-related differences can best be improved by accounting for additional sources of variability other than those related to inherent wideband pilot response randomness (i.e., "remnant"). Furthermore, there is some indication that the threshold associated with acquisition of information from the panel-mounted airspeed indicator is more closely related to visual resolution limitations than to an indifference threshold based on the distance between adjacent calibration markings.

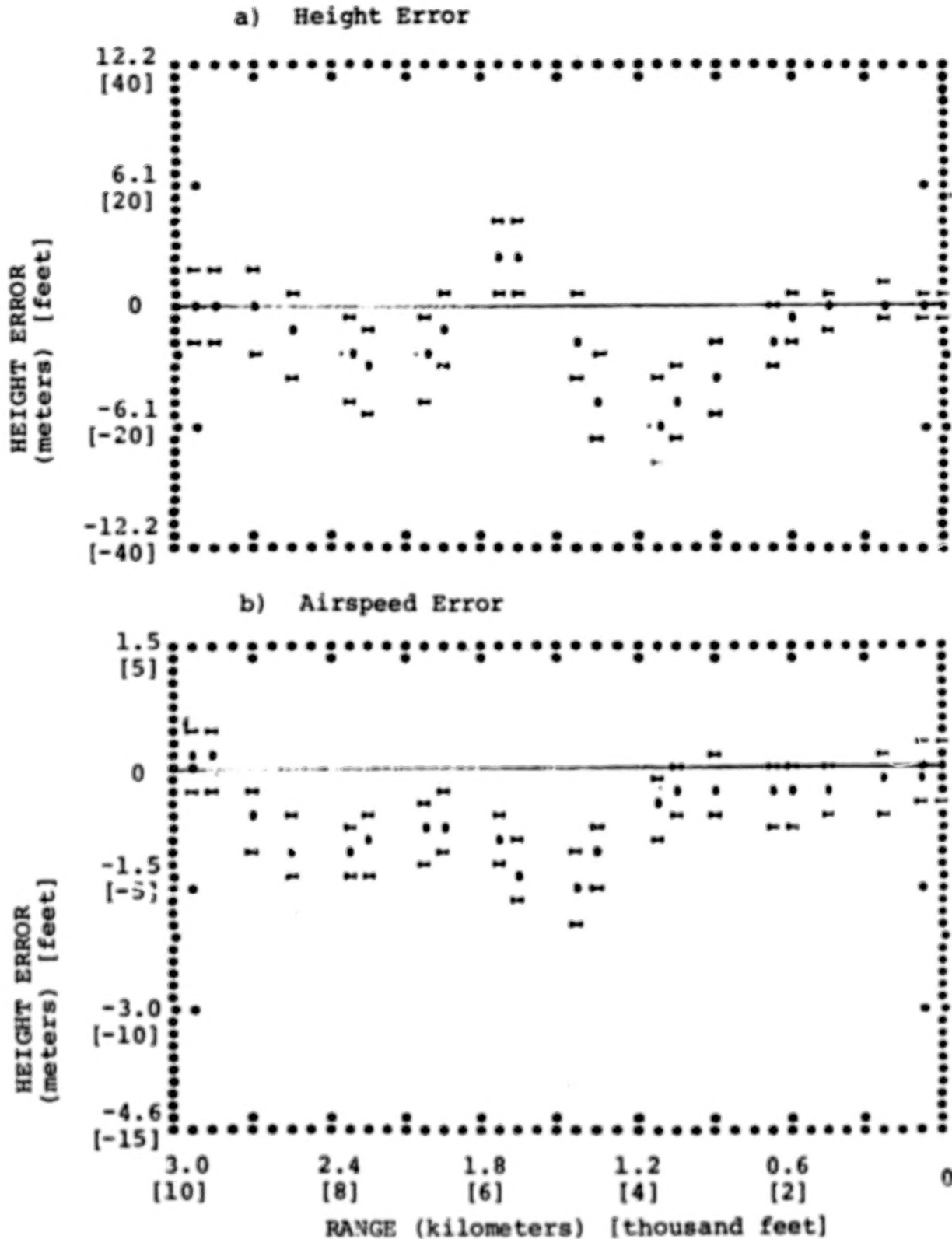


Figure 37. Predicted Response Variability for Increased Driving Noise

Attitude CWS, Advanced Display, Shear 3

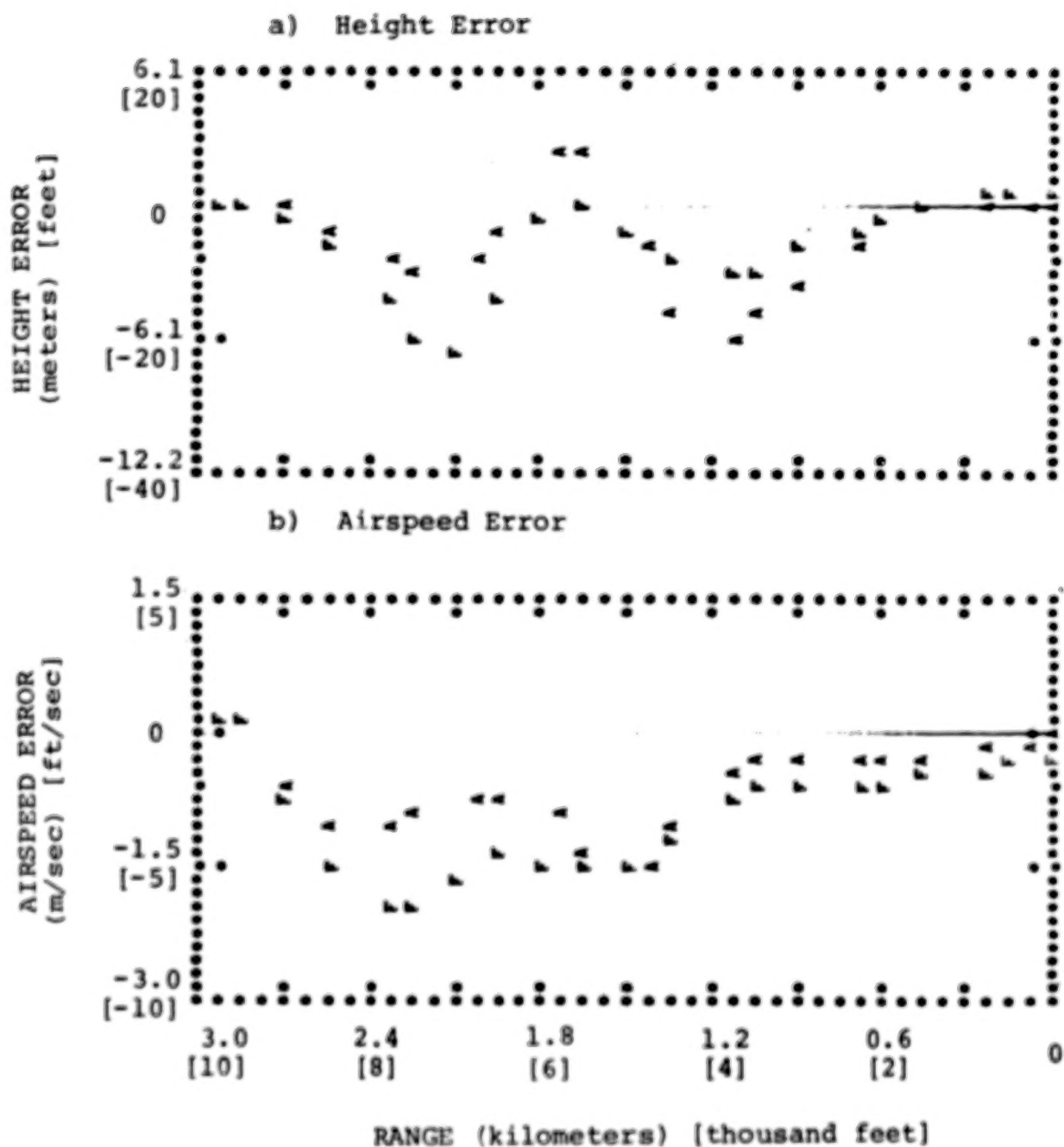


Figure 38. Effect of Display on Predicted Mean Error for Increased Driving Noise

Attitude CWS, Shear 3

A = advanced display, F = flight director

5. SUMMARY AND CONCLUSIONS

In general, performance trends predicted by the model were confirmed experimentally. Experimental and analytical results both indicated superiority of the "advanced" display with respect to regulation of height and airspeed errors. Velocity steering allowed tighter regulation of height errors, but control parameters had little influence on airspeed regulation. Model analysis indicated that display-related differences could be ascribed to differences in the quality of speed-related information provided by the two displays.

Predictions were most accurate with regard to display- and control-related differences in the total swing of the mean error over the course of the approach, and least accurate with regard to response variability and absolute levels of mean error. Experimental run-to-run variability was from 2 to 3 times as great as predicted for both height and speed errors, and mean errors tended to be less negative (or more positive) than predicted. The relatively large experimental variability may have been, in part, a result of keeping the data base small to prevent the pilot's learning of the shear profile. In addition, there appeared to be a tendency for the pilots to fly high and/or fast on some trials and not on others, a factor that could contribute to predictive inaccuracies.

Post-experimental analysis was performed to explore the influence of certain model parameters on predictive accuracy. On the whole, it appears that the match to the experimental display-related differences can best be improved by accounting for additional sources of variability other than those related to wideband pilot response randomness. There is also some

indication that an overly pessimistic assumption regarding the threshold on airspeed perception was made for the director configuration.

In order to validate the model and to facilitate interpretation of experimental results, most of the analysis conducted in this study was in direct support of the specific experiments performed concurrently at NASA-LRC. Nevertheless, one of the most advantageous uses of the model is to explore interesting alternatives and answer questions that have not been (or cannot easily be) addressed directly in manned simulation experiments.

Within the constraints of the study program, some attempt was made to perform such extrapolation with the model. For example, the consequence of accompanying the flight director display with a suitably sensitive indicator of airspeed error was explored. From this analysis we concluded that display-related differences were caused primarily by differences in the quality of the presentation of speed-related information.

Model analysis was also performed to determine the potential benefit of providing the pilot with better information regarding the current state of the wind under the assumption that the pilot does not attempt to predict the future course of the wind. No performance improvement was predicted for this configuration. Thus, if display augmentation is to benefit performance, the pilot will have to attempt to estimate the shear aspects (i.e., rate of change) of the wind, and a predictive display of the wind may be required as well.

Using the pilot/vehicle model, we can address questions relating both to the pilot's conception of the behavior of the wind as well as to the wind information explicitly displayed. For example, we can assume that the pilot knows that the wind will change with altitude (and thus with time) in a smooth manner,* and we can explore the consequences of displaying (a) the same variables displayed in this study, (b) additional variables relating to the current wind state, and (c) additional variables relating to the rate-of-change of wind. Furthermore, one can explore the interaction of these factors with the type and severity of shear. Additional factors that can be explored are the relation between performance and workload for candidate controls and displays, as well as the utility of motion cues in detection of windshears.

One of the difficulties associated with experimentation concerning windshear response is the possibility of the test pilots learning the specific experimental shear profiles. To maintain relevance to operational situations, learning is kept to a minimum by restricting the size of the data base; unfortunately, this technique also limits the reliability of the results. In short, there is a fundamental problem concerning experiments with nonrandom inputs for which no obvious solution exists. In a situation of this sort, it is entirely possible that model results will be more reliable than experimental results, since the state of learning is a model parameter that can be controlled.

*The pilot was assumed to have a zero-order (constant value) model of the wind in this study.

Another area in which the pilot/vehicle model may be profitably applied is in the design of simulation experiments. For example, in future studies, one might wish to explore response behavior in shear environments in which height and speed errors are marginally acceptable (or unacceptable). The model would be used prior to experimentation to identify interesting shear environments, as well as to identify control and display modifications that are likely to influence response capabilities.

In conclusion, the model employed in this study has been validated with regard to its ability to predict important performance trends related to controls and displays in wind-shear environments. Because of the operational necessity of understanding performance in windshears, we suggest that the pilot/vehicle model be applied further to aid in the design of simulation experiments and to explore a variety of factors that cannot be readily studied in the laboratory. While we cannot guarantee accurate predictions of absolute performance levels at this stage of model development, the model should provide reliable indications of the nature of performance and workload improvements that can be achieved with candidate controls and displays in a variety of windshear environments.

APPENDIX

MODEL FOR PILOT RESPONSE TO NONRANDOM INPUTS

A.1 Introduction

The "optimal control" pilot/vehicle model that has been used in the first phase of this study program [1] and in numerous other studies assumes that the pilot performs the function of optimal state estimation as well as optimal control.* In order to be truly optimal, the estimator (implemented as a Kalman filter) should contain a model of the system (pilot's "internal model") that accounts for all correlations between state variables. Thus, the internal model should contain an accurate representation of system dynamics (including noise-shaping filters to represent, say, gust spectra); in addition, we usually assume that the pilot knows the statistics--but not the actual time histories--of all random inputs.

Certain modifications have to be made to this model when we wish to consider tasks in which the inputs are nonrandom (deterministic), rather than zero-mean random noise. In this case, we must make certain assumptions about the pilot's knowledge of the input structure--assumptions that have a strong influence on model predictions.

*Readers who do not have a working knowledge of the optimal-control pilot/vehicle model are directed to Levison and Baron [1] and to references given in that document.

The most straightforward application of the optimal-control model would be to assume that the pilot knows the structure of the input. To predict the response to, say, a windshear under this assumption, we would approximate the shear profile as the transient output of a linear filter with appropriate initial conditions. The dynamics of this filter would be included in the pilot's internal model, and his estimation task (with respect to the windshear) would simply be to estimate the instantaneous values of the shear state variables. Previous experience with the model indicates that this assumption would allow the (mathematical) pilot to estimate the shear states early in the "flight" and, therefore, to predict and compensate for the shear profile for the remainder of the flight.

This assumption of perfect knowledge of structure is clearly too optimistic for a pilot encountering a windshear in actual flight. Because of the high degree of variability associated with windshears [3], it is unlikely a pilot will encounter a specific shear profile more than once even though he frequently flies in shear environments.

Taking the opposite extreme, one could assume that the pilot knows nothing about the shear and fails to allow for the possibility that a shear might be present. We would model this hypothesis by omitting shear-related state variables from the internal model contained in the Kalman filter. In this case, the estimator would operate as if there were only zero-mean random disturbances present and would not attempt to estimate the nonrandom disturbance.

The extent to which this latter assumption would lead to unreasonable model predictions would depend on the total (simulated) wind environment. If significant wind gusts were assumed to be present, the "pilot" would most likely reduce the effects of the nonrandom input in the course of responding to the random inputs. On the other hand, if there were only minimal random disturbances (as was the case with the experiments performed in conjunction with this study), the "pilot" would basically fail to respond, and the aircraft would drift considerably off course. While this assumption may be appropriate in certain extreme situations, it is overly pessimistic for pilots (such as those participating in the LRC study) who have been trained in actual or simulated shear environments.

As explained in the main text, we adopted for this study a simple representation of the pilot's knowledge of the windshear; specifically, we assumed no knowledge of the shear structure, only the knowledge that a non zero-mean wind might exist. We assumed that the pilot would not try to anticipate changes in the wind, but would, at best, attempt to estimate the current wind vector. This level of knowledge was modeled simply by implementing a stepwise-constant representation of the wind.

The pilot-vehicle model was modified to reflect the following assumptions concerning pilot behavior in a nonrandom input environment:

1. The pilot looks for biases (i.e., nonzero means) in the residuals, where "residuals" is, in essence, the difference between the anticipated and actual value of a display variable. (In a situation in which the pilot's estimator accounts for all correlations among state variables, the residuals will be white noise processes.)

2. The pilot decides whether or not the apparent bias on the residuals is sufficiently large to warrant special action.
3. If such action is warranted, the pilot increments the uncertainty associated with relevant state variables, where "uncertainty" is synonymous with the covariance of the estimation error, Σ . This increment is in addition to the change in Σ that is determined by the rules for optimal filtering. As a (mathematical) consequence of incrementing Σ , the pilot is forced to rely more heavily on recent measurements and less heavily on predicted system behavior--a reasonable strategy for a pilot to adopt when he has reason to doubt his internal model of the situation.

This modeling philosophy differs in certain respects from that adopted in previous studies of human controller behavior involving nonrandom inputs [4]. In those studies, we simply assumed that the pilot's uncertainty would grow in proportion to the activity of the input (either magnitude or rate-of-change), and we incremented uncertainty for only those states corresponding to the nonrandom inputs. Although this approach has yielded good correspondence with experimental results, the approach used in the current study has a firmer physical basis and is perhaps more consistent with optimal estimation theory. Specifically, it seems more reasonable to model the pilot's response to variables that he can readily perceive (discrepancies between anticipated and observed display quantities) than to variables that are unknown to him (amplitudes and rates of inputs not displayed).

A.2 Conceptual Model

Before describing the implementation of the procedure for incrementing the error covariance, it is instructive to discuss in more detail the procedure that we assume the pilot to adopt when dealing with nonrandom inputs. It should be pointed out that this conceptual model has been designed partly to be compatible with notions of optimality and partly to lead to a tractable and relatively simple modification of the existing model. As is the case with Kalman filtering and other aspects of the model, this submodel does not necessarily reflect actual mental processes generated by the human controller; rather, the model is intended to lead to predictions of pilot response behavior that correspond well with experimental measurements.

Because we are dealing with a time-varying situation, rather than continuous steady-state, the model has been implemented in a discrete-time format. Therefore, references to time will be to the discrete time index "k" rather than to continuous time.

We assume that the pilot adopts the following model for the residual at time index (k):

$$\underline{r}(k) = \underline{C}\phi[\underline{\tilde{x}}(k-1) + \underline{\Delta x}(k-1)] + v_y(k) \quad (1)$$

where $\underline{r}(k)$ is the residual, \underline{C} the matrix relating displayed variables to state variables, ϕ the "transition matrix" relating state variables at index "k" to the state at the preceding time index, $\underline{\tilde{x}}$ the estimation error, and $\underline{\Delta x}$ an assumed bias error in the estimate. Except for the term $\underline{\Delta x}$, this expression describes the relationship between the residual and other quantities in a system involving optimal state estimation [5].

Now, the pilot cannot know the estimation error at any given time. (If he did, he could correct his estimate and reduce the error to zero.) He expects, however, that the residuals will be uncorrelated and have zero mean in a system driven by zero-mean white noise processes. We assume that the pilot looks for a consistent bias in the residuals, which he attributes to a bias error in his state estimates, represented by the quantity Δx .

To determine whether or not the residual contains a consistent bias, we assume that the pilot, in effect, computes a short-term average of the residual, which we designate as \underline{r}^* . This averaging process is represented in the model as a first-order filtering operation on the sequence $\underline{r}(k)$. The time constant of this filter, T_f , introduces a new pilot parameter to the model.

The pilot must decide whether or not the apparent bias is sufficiently large to warrant special action. (That is, is \underline{r}^* of sufficient magnitude to reject the hypothesis that it is a sample of a zero-mean random process?) To make this decision, the pilot tests \underline{r}^* against a Gaussian probability density having zero mean and variance σ_1 , where σ_1 is the variance that the residuals would have if, in fact, the system had no nonrandom inputs.

We assume that the pilot adopts a "decision window" equal to some number of standard deviations; if \underline{r}^* is outside this window, he rejects the null hypothesis and assumes that a nonrandom input is present. We further assume that the pilot individually tests each element \underline{r}^* against its theoretical standard

deviation, and rejects the null hypothesis if at least one element fails the test. Thus, the pilot decides that random inputs are present if

$$\frac{\underline{r}^*_{i}}{\sigma_i} > W \quad (2)$$

for one or more values of the index "i"; otherwise, he assumes only zero-mean inputs are present. The decision window W introduces another new pilot-related model parameter.

Once the pilot detects the presence of a nonrandom input, he must make some adjustment to his estimator in order to be able to estimate the value(s) of the nonrandom input(s). There are basically two strategies he can follow: he can attempt to correct his estimate directly based on \underline{r}^* , or he can use \underline{r}^* as a basis for increasing his uncertainty so that his optimal estimation will, over a period of time, give him an estimate of the nonrandom inputs. We assume that the pilot adopts the latter strategy of "opening the filter".

To determine the quantity of $\Delta \underline{E}$ by which to increment the estimation error covariance, the pilot assumes that the filtered residual is due entirely to a bias error in his estimate. Thus, from Eq(1)

$$\underline{r}^* \approx \underline{C} \underline{\Phi} (\Delta \underline{x}) \quad (3)$$

The outer product of \underline{r}^* is thus

$$\underline{r}^* \underline{r}^{*'} = \underline{C} \underline{\Phi} (\Delta \underline{x} \Delta \underline{x}') (\underline{C} \underline{\Phi})' \quad (4)$$

We assume that the pilot will update his error covariance by the outer product of the bias term Δx ; that is $\Delta E = \Delta x \Delta x'$. From eq (3) we obtain,

$$\Delta E = (\underline{C}\phi)^+ (\underline{r}^* \underline{r}^{*'}) (\underline{C}\phi)^+ \quad (5)$$

where "+" indicates the pseudo-inverse operation [6].

The operator is assumed to increment his estimation error covariance according to the above expression, with the following qualification:

1. The increment is performed only when warranted by the test of eq (2); otherwise, the covariance matrix is updated solely according to the rules for optimal filtering.
2. The operator does not increment the full covariance matrix, but only the elements corresponding to state variables that the operator expects to be disturbed by nonrandom inputs. For example, a pilot anticipating windshears may construct an internal model of the system that contains state variables specifically associated with the windshear and increment uncertainty only on those states. Another pilot may construct a model that lacks a representation of the windshear and may increment uncertainty on all vehicle states. The set of states to be affected in this manner introduces a third (and final) pilot-related parameter.
3. The operator does not use the full set of residuals to increment the error covariance, but uses only those terms that are most sensitive to bias errors in the state estimates. (This qualification was introduced to minimize the incidence of numerical difficulties in performing the required matrix-inverse operations.)

A.3 Model Implementation

We now describe the way in which the above conceptual model was implemented in the computerized pilot-vehicle model used in this study. Because the model is a statistical model (i.e., each trial solution yields a predicted mean and variance - not a sample time history), operations were performed on either expected values (means) or variances.

The expected value of the filtered residual was computed as

$$\underline{r}^*(k) = h \underline{r}^*(k-1) + (1-h) \underline{r}(k-1) \quad (6)$$

where $h = e^{-T/T_f}$, T is the update interval adopted for obtaining a problem solution, and T_f is the time-constant of the first-order averaging filter. For this study, values of 1 and 2 seconds were adopted for T and T_f , respectively.

The expected value of the (unfiltered) residual \underline{r} was updated according to

$$\underline{r}(k) = \underline{C} \tilde{\underline{x}}(k) \quad (7)$$

where, in this operation, $\tilde{\underline{x}}(k)$ represents the mean estimation error at time index k . The diagonal elements of the covariance matrix σ^2_i were computed as

$$\sigma^2_i(k) = h^2 \sigma^2_i(k-1) + (1-h)^2 \left\{ \frac{VY_i(k)}{T} + \underline{C} \underline{\Sigma}(k) \underline{C}' \right\} \quad (8)$$

where $VY_i(k)$ is the covariance of the observation noise associated with the i^{th} display element.

The test indicated in eq (2) was performed for each element of the \mathbf{r}^* vector. For the element r_i^* that was most deviant (i.e., greatest number of standard deviations from zero) the program computed the probability P that a signal having a mean r_i^* and variance σ_i^2 would be outside the window delimited by $\pm W$. This probability was considered to be (approximately) the probability that the pilot would, at a given time step, decide that a nonrandom input was present and increment his error covariance.

For the model runs shown in the main body of this report, the window W was chosen to be two standard deviations.

As noted above, the increment of the error covariance was computed for a selected set of state variables and a selected set of output variables. The computer program was designed to let the subset of state variables be selected at runtime by the user, according to whatever assumption seemed appropriate with regard to actual pilot behavior.

The following three hypotheses were explored during preliminary analysis:

1. Being unaware of the possibility of a windshear; the pilot excludes corresponding state variables from his model of the system and associates uncertainty with all vehicle states.

TABLE OF CONTENTS

<u>Section</u>	<u>Page</u>
SUMMARY	1 1/A10
1. INTRODUCTION	2 1/A11
2. PROBLEM DEFINITION	4 1/A13
2.1 Description of the Flight Task	4 1/A13
2.2 Control Wheel Steering	4 1/A13
2.3 Displays	5 1/A14
2.4 Simulated Winds	9 1/B4
3. MODEL ANALYSIS	13 1/B8
3.1 Pilot-Related Model Parameters	13 1/B8
3.2 Wind Model	19 1/B14
3.3 Model Predictions	22 1/C3
4 EXPERIMENTAL STUDY	49 1/E2
4.1 Description of Experiments	49 1/E2
4.2 Data Analysis Procedures	50 1/E3
4.3 Comparison of Predicted and Experimental Results	52 1/E5
4.4 Post-Experimental Model Analysis	65 1/F4
5 SUMMARY AND CONCLUSIONS	76 1/G1
APPENDIX	A1 1/G5
Model for Pilot Response to Nonrandom Inputs	
REFERENCES	

2. The pilot includes wind states in his internal model and associates uncertainty with both wind states and vehicle states.
3. The pilot includes wind states in his internal model and increments elements of the covariance matrix corresponding to those states only.

Model predictions generated according to the first hypothesis showed height errors becoming excessively large near touchdown. Partly because of this result, and partly because this assumption seemed on its face to be unduly pessimistic for a knowledgeable pilot, this assumption was discarded.

Results with assumptions 2 and 3 were quite similar, leaving little basis to choose between them. The decision was made to perform the bulk of the model analysis according to the second hypothesis.

The subset of element of \mathbf{r}^* to use in computing $\Delta\mathbf{z}$ was determined by finding for each state variable used in this computation, the component of \mathbf{r}^* most sensitive to a bias error in the state estimate. In computing this sensitivity, the mean residual was normalized with respect to its (theoretical) standard deviation. Thus, for each element of \mathbf{r}^* , the program computed

$$\frac{\partial (r_i^* / \sigma_i)}{\partial \Delta x_j} = \frac{[C\Phi]_{ij}}{\sigma_i}$$

where the index "i" was taken over all display quantities and the index "j" over the subset of state variables as defined above.

The modified \underline{r}^* vector consisted only of components that were maximally sensitive for each index "j". Thus, if NX_u was the number of states considered in determining $\Delta \underline{\Sigma}$, the dimension of the modified \underline{r}^* vector was NX_u or less, - typically less, since it was often the case that biases in two or more states had maximal influence on the same display variable.

In order to reflect the assumption that the pilot would increment his uncertainty only when he detected consistent bias in the residuals, the increment added at each time step of the problem solution was multiplied by the probability P that the most deviant residual would be outside the decision window. Thus, the increment was implemented as

$$\Delta \underline{\Sigma}_s = P [\underline{C}\Phi]_s^+ [\underline{r}^* \underline{r}^{*T}]_x [\underline{C}\Phi]_s^+ \quad (10)$$

where the subscript "s" signifies that the computation was made with respect to a selected subset of state and display variables.

REFERENCES

1. Levison, W. H. and S. Baron, "Analytic and Experimental Evaluation of Display and Control Concepts for a Terminal Configured vehicle," BBN Report No. 3270, Bolt Beranek and Newman, Inc., Cambridge, Mass., July 1976.
2. Chalk, C. R.; T. P. Neal, T. M. Harris, F. E. Pritchard, and R. J. Woodcock: "Background Information and User Guide for MIL-F-8785B(ASG), "Military Specification - Flying Qualities of Piloted Airplanes." AFFDL-TR-69-72, U.S. Air Force, Aug. 1969. (Available from DDC as AD 860 856.)
3. Foxworth, T. G. and H. F. Marthinsen, "Another Look at Landing and Stopping Criteria," AIAA Paper No. 74-956, AIAA 6th Aircraft Design Flight Test and Operations Meeting, Los Angeles, California, August 12-14, 1974.
4. Baron, S. and W. H. Levison, "Analysis and Modelling Human Performance in AAA Tracking," BBN Report No. 2557, Bolt Beranek and Newman Inc., Cambridge, Mass., March 1974.
5. Grenville, T. N. E., "Some Applications of the Pseudoinverse of a Matrix", SIAM REVIEW, Vol. 2, pp. 15-22, January 1960.
6. Gelb, A. (ed), Applied Optimal Control, M.I.T. Press, 1974.

1. Report No. NASA CR-3034		2. Government Accession No.		3. Recipient's Catalog No.	
4. Title and Subtitle Analysis and In-Simulator Evaluation of Display and Control Concepts for a Terminal Configured Vehicle in Final Approach in a Wind-shear Environment				5. Report Date August 1978	
				6. Performing Organization Code	
7. Author(s) William H. Levison				8. Performing Organization Report No.	
9. Performing Organization Name and Address Bolt Beranek and Newman Inc. Cambridge, MA 02138				10. Work Unit No.	
				11. Contract or Grant No. NAS1-13842	
12. Sponsoring Agency Name and Address National Aeronautics & Space Administration Washington, DC 20546				13. Type of Report and Period Covered Contractor Report	
				14. Sponsoring Agency Code	
15. Supplementary Notes NASA Technical Monitor: George G. Steinmetz Final Report					
16. Abstract This report concerns the analysis of display-control configurations for the Terminal Configured Vehicle in approach to landing situations. A pilot/vehicle model was used to compare with a real-time simulation study. Model results are presented and extended for the approach task during wind shear and random turbulence environments. In general, model results of performance trends matched those obtained experimentally.					
17. Key Words (Suggested by Author(s)) Pilot/Vehicle Model, Displays, Wind Shears				18. Distribution Statement Unclassified - Unlimited Subject Category-63	
19. Security Classif. (of this report) Unclassified		20. Security Classif. (of this page) Unclassified		21. No. of Pages 99	
				22. Price* \$6.00	

90

50

2

END

NOV 28 1978